Energy-Efficient Power Allocation in Cognitive Radio Systems With Imperfect Spectrum Sensing

Gozde Ozcan, M. Cenk Gursoy, Nghi Tran, and Jian Tang, *Senior Member, IEEE*

***Abstract*— This paper studies energy-efficient power allocation schemes for secondary users in sensing-based spectrum sharing cognitive radio systems. It is assumed that secondary users first perform channel sensing possibly with errors and then initiate data transmission with different power levels based on sensing decisions. In this setting, the optimization problem is to maximize energy efficiency (EE) subject to peak/average transmission power constraints and peak/average interference constraints. By exploiting the quasi-concave property of the EE maximization problem, the original problem is transformed into an equivalent parameterized concave problem, and an iterative power allocation algorithm based on Dinkelbach's method is proposed. The optimal power levels are identified in the presence of different levels of channel side information (CSI) regarding the transmission and interference links at the secondary transmitter, namely, perfect CSI of both transmission and interference links, perfect CSI of the transmission link, imperfect CSI of the interference link, imperfect CSI of both links, or only statistical CSI of both links. Through numerical results, the impact of sensing performance, different types of CSI availability, and transmit and interference power constraints on the EE of the secondary users is analyzed.**

***Index Terms*— Dinkelbach's method, energy efficiency, imperfect/perfect/statistical CSI, imperfect spectrum sensing, interference power constraint, power allocation, probability of detection, probability of false alarm, transmit power constraint.**

I. Introduction

DRIVEN by the emergence of new applications, growing demand for high data rates and increased number of users, energy consumption of wireless systems has gradually increased, leading to high levels of greenhouse gas emissions, consequent environmental concerns and high energy prices and operating costs. Therefore, optimal and efficient use of energy resources with the goal of reducing costs and minimizing the carbon footprint of wireless systems is of paramount importance, and energy-efficient design has become a vital consideration in wireless communications from the perspective of green operation. In addition, bandwidth bottleneck is a critical concern in wireless services since there are only limited spectral resources to accommodate multiple users and multiple wireless applications operating simultaneously. Despite this fact, the report released by the Federal Communication Commission showed that a large portion of the radio spectrum is not fully utilized most of the time [1]. Hence, inefficiency in the spectrum usage opens the possibility for a new communication paradigm, called as cognitive radio [2], [3]. In cognitive radio systems, unlicensed (cognitive or secondary) users are able to opportunistically access the frequency bands allocated to the licensed (primary) users as long as interference inflicted on primary users is limited below tolerable levels. Hence, cognitive radio leads to the dynamic and more efficient utilization of the available spectrum.

Motivated by the energy efficiency (EE) and spectral efficiency (SE) requirements and the need to address them jointly, we in this paper study EE in cognitive radio systems. More specifically, we investigate energy-efficient power allocation strategies in a practical setting with imperfect spectrum sensing.

A. Literature Review

EE in cognitive radio systems has been recently addressed in [4]–[12]. For instance, the authors in [4] highlighted the benefits of cognitive radio systems for green wireless communications. The study in [5] mainly focused on SE and EE of cognitive cellular networks in 5G mobile communication systems. The optimization of various parameters affecting the EE of the secondary users such as sensing strategies [6], sensing time and transmission duration [7] was studied. In addition, several recent works investigated power allocation/control to maximize the EE in different settings. In particular, the objectives of the power optimization problems include the EE of the secondary user [8], [9], minimum EE among all secondary users [10] and sum EE of secondary users [10]–[12]. In the EE analysis of the work in [6], [7], and [10], secondary users are assumed to transmit only when the channel is sensed as idle, which is called as opportunistic spectrum access scheme. On the other hand, the studies in [8], [9], [11], and [12] considered underlay transmission scheme in which the secondary users always share the spectrum with primary users without performing channel sensing. In order to further increase the transmission opportunities of the secondary users, sensing-based spectrum sharing was proposed [13] which allows the secondary users to transmit under both idle and busy sensing decisions while adapting the transmission power according to the sensing results. For the sensing-based spectrum sharing scheme, throughput-efficient

Manuscript received February 1, 2016; revised May 16, 2016 and September 16, 2016; accepted October 16, 2016. Date of publication October 25, 2016; date of current version December 29, 2016. This work was supported by the National Science Foundation under Grant CNS-1443966, Grant ECCS-1443994, and Grant CCF-1618615. *(Corresponding author: Gozde Ozcan.)*

G. Ozcan, M. C. Gursoy, and J. Tang are with the Department of Electrical Engineering and Computer Science, Syracuse University, Syracuse, NY 13244 USA (e-mail: gozcan@syr.edu; mcgursoy@syr.edu; jtang02@syr.edu).

N. Tran is with the Department of Electrical and Computer Engineering, The University of Akron, Akron, OH 44325 USA (e-mail: nghi.tran@uakron.edu).

Color versions of one or more of the figures in this paper are available online at http://ieeexplore.ieee.org.

Digital Object Identifier 10.1109/JSAC.2016.2621399

power allocation strategies were determined for a single carrier system subject to average transmit and interference power constraints [13] and for a multicarrier system subject to either average transmit and average interference power constraints [14] or average transmit power and primary user rate loss constraints [15]. However, energy-efficient power allocation schemes have not been sufficiently addressed in sensing-based spectrum sharing cognitive radio systems.

It should be noted that the aforementioned works rely on the availability of perfect channel side information (CSI) of the transmission link between the secondary transmitter and the secondary receiver, and the interference link between the secondary transmitter and the primary receiver, which is hard to obtain in practice due to the random nature of wireless channels, limited training sequences, delay in feedback channels, lack of cooperation between the primary users and the secondary users, and other practical factors. With this motivation, the impact of imperfect CSI of only the transmission link [16], of only the interference link [17], [18], and of both the transmission and interference links [19] on the EE performance of cognitive radio systems was studied.

B. Main Contributions

Similar to the studies in [13]–[15], we consider that the secondary users employ a sensing-based spectrum sharing transmission scheme. In this setting, we focus on adapting the transmission power according to the sensing results and determining the optimal power allocation schemes to maximize the EE of secondary users under constraints on both the transmission and interference power levels. The main contributions of this paper are summarized below:

- We formulate the EE maximization problem subject to peak/average transmit power constraints and peak/average interference constraint in the presence of imperfect sensing results. In particular, EE is defined as the ratio of the achievable rate over the total power expenditure including circuit power consumption. We explicitly show in the formulations the dependence of the achievable rate and energy efficiency on sensing performance and reliability.
- After transforming the EE maximization problem into an equivalent concave form, we apply Dinkelbach's method to find the optimal power allocation schemes. Subsequently, we develop an efficient low-complexity power allocation algorithm for given channel fading coefficients of the transmission link between the secondary transmitter-receiver pair and of the interference link between the secondary transmitter and the primary receiver.
- We study the impact of different levels of channel knowledge regarding the transmission and interference links on the optimal power allocation and the resulting EE performance of secondary users. In practice, perfect CSI is difficult to obtain due to the inherently time-varying nature of wireless channels, delay, noise and limited bandwidth in feedback channels and other factors. Therefore, our proposed power allocation schemes obtained under imperfect CSI are useful in practical settings and give insight about the impact of channel uncertainty on the system performance. At the same time, the EE in the presence of perfect CSI of the transmission and interference links serves as a baseline to compare the performances attained under the assumption of imperfect and statistical CSI of both links.
- We also investigate the effects of imperfect sensing decisions, and the constraints on both transmit and interference power on the EE of secondary users.

The remainder of the paper is organized as follows. Section II introduces the system model and defines the EE of secondary users in the presence of imperfect sensing results. In Section III, EE maximization problems subject to transmit and interference power constraints in the presence of imperfect sensing results and different levels of CSI regarding the transmission and interference links are formulated and the corresponding optimal power allocation schemes are derived. Subsequently, numerical results are presented and discussed in Section IV before giving the main concluding remarks in Section V.

II. System Model

We consider a sensing-based spectrum sharing cognitive radio system in which a secondary transmitter-receiver pair utilizes the spectrum holes in the licensed bands of the primary users. The term "spectrum holes" denotes underutilized frequency intervals at a particular time and certain location. In order to detect the spectrum holes, secondary users initially perform channel sensing over a duration of τ. It is assumed that secondary users employ frames of duration T. Hence, data transmission is performed in the remaining duration of $T-\tau$.

A. Channel Sensing

Spectrum sensing can be formulated as a hypothesis testing problem in which there are two hypotheses based on whether primary users are active or inactive over the channel, denoted by $\mathcal{H}_0$ and $\mathcal{H}_1$, respectively. Many spectrum sensing methods have been studied in the literature (see e.g., [20], [21], and references therein) including matched filter detection, energy detection and cyclostationary feature detection. Each method has its own advantages and disadvantages. However, all sensing methods are inevitably subject to errors in the form of false alarms and miss detections due to possibly low signal-to-noise ratio (SNR) levels of primary users, noise uncertainty, multipath fading and shadowing in wireless channels. Therefore, we consider that spectrum sensing is performed imperfectly with possible errors, and sensing performance depends on the sensing method only through detection and false alarm probabilities. As a result, any sensing method can be employed in the rest of the analysis. Let $\hat{\mathcal{H}}_1$ and $\hat{\mathcal{H}}_0$ denote the sensing decisions that the channel is occupied and not occupied by the primary users, respectively. Hence, by conditioning on the true hypotheses, the detection and false-alarm probabilities are defined, respectively, as follows:

$$\mathscr{P}_{\mathrm{d}} = \Pr\{\hat{\mathcal{H}}_1|\mathcal{H}_1\}, \tag{1}$$

$$\mathscr{P}_{\mathrm{f}} = \Pr\{\hat{\mathcal{H}}_1|\mathcal{H}_0\}. \tag{2}$$

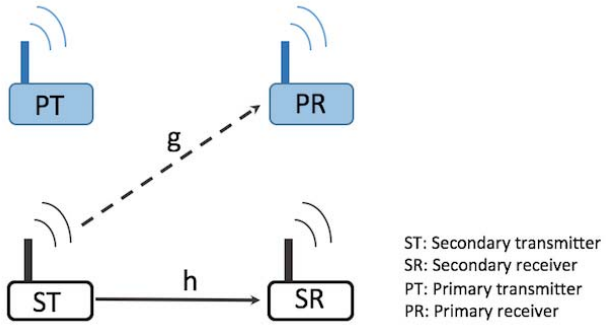

Fig. 1. System model.

Then, the conditional probabilities of idle sensing decision given the true hypotheses can be expressed as

$$\Pr\{\hat{\mathcal{H}}_0|\mathcal{H}_1\} = 1 - \mathscr{P}_{\rm d}, \tag{3}$$

$$Pr\{\hat{\mathcal{H}}_0|\mathcal{H}_0\} = 1 - \mathscr{P}_{\rm f}. \tag{4}$$

B. Cognitive Radio Channel Model

Following channel sensing, the secondary users initiate data transmission. The channel is considered to be block flat-fading channel in which the fading coefficients stay the same in one frame duration and vary independently from one frame to another. Secondary users are assumed to transmit under both idle and busy sensing decisions. Therefore, by considering the true nature of the primary user activity together with the channel sensing decisions, the four possible channel input-output relations between the secondary transmitter-receiver pair can be expressed as follows:

$$y_i = \begin{cases} hx_{0,i} + n_i & \text{if } (\mathcal{H}_0, \hat{\mathcal{H}}_0) \\ hx_{1,i} + n_i & \text{if } (\mathcal{H}_0, \hat{\mathcal{H}}_1) \\ hx_{0,i} + n_i + s_i & \text{if } (\mathcal{H}_1, \hat{\mathcal{H}}_0) \\ hx_{1,i} + n_i + s_i & \text{if } (\mathcal{H}_1, \hat{\mathcal{H}}_1), \end{cases} \tag{5}$$

where $i = 1, \ldots, T - \tau$. Above, x and y are the transmitted and received signals, respectively and h is the channel fading coefficient of the transmission link between the secondary transmitter and the secondary receiver, which is assumed to be Gaussian distributed with mean zero and variance σ_h^2. In addition, n_i and s_i denote the additive noise and the primary users' received faded signal. Both $\{n_i\}$ and $\{s_i\}$ are assumed to be independent and identically distributed circularly-symmetric, zero-mean Gaussian sequences with variances N_0 and σ_s^2, respectively. Moreover, the subscripts 0 and 1 in the transmitted signal indicate the transmission power levels of the secondary users. More specifically, the average power level is $P_0(g, h)$ if the channel is detected to be idle while it is $P_1(g, h)$ if the channel is detected to be busy. Also, g denotes the channel fading coefficient of the interference link between the secondary transmitter and the primary receiver. System model is depicted in Fig. 1.

Based on the input-output relation in (5), the additive disturbance is given by

$$w_i = \begin{cases} n_i & \text{if } \mathcal{H}_0 \text{ is true} \\ n_i + s_i & \text{if } \mathcal{H}_1 \text{ is true.} \end{cases} \tag{6}$$

In this setting, achievable rates of secondary users can be characterized by assuming Gaussian input and considering the input-output mutual information $I(x; y|h, \hat{\mathcal{H}})$ given the fading coefficient h and sensing decision $\hat{\mathcal{H}}$:

$$\begin{aligned} R_G &= \frac{T-\tau}{T} I(x; y|h, \hat{\mathcal{H}}) \\ &= \frac{T-\tau}{T}\Big[\Pr\{\hat{\mathcal{H}}_0\} I(x_0; y|h, \hat{\mathcal{H}}_0) + \Pr\{\hat{\mathcal{H}}_1\} I(x_1; y|h, \hat{\mathcal{H}}_1) \Big] \\ &= \frac{T-\tau}{T} \Pr(\hat{\mathcal{H}}_0)\big[h(y|h, \hat{\mathcal{H}}_0) - h(y|x_0, h, \hat{\mathcal{H}}_0)\big] \\ &\quad + \frac{T-\tau}{T} \Pr(\hat{\mathcal{H}}_1)(h(y|h, \hat{\mathcal{H}}_1) - h(y|x_1, h, \hat{\mathcal{H}}_1)), \\ &= \frac{T-\tau}{T} \Pr(\hat{\mathcal{H}}_0)\big[h(y|h, \hat{\mathcal{H}}_0) - h(w|h, \hat{\mathcal{H}}_0)\big] \\ &\quad + \frac{T-\tau}{T} \Pr(\hat{\mathcal{H}}_1)\big[h(y|h, \hat{\mathcal{H}}_1) - h(w|h, \hat{\mathcal{H}}_1)\big], \end{aligned} \tag{7}$$

where $h(.)$ denotes the differential entropy. Due to imperfect sensing results, the additive disturbance, w, follows a Gaussian mixture distribution and the differential entropy of Gaussian mixture density does not admit a closed-form expression. Hence, we do not have an explicit expression for R_G with which we can identify the energy efficiency and obtain the optimal power allocation strategies. However, a closed-form achievable rate expression for secondary users can be obtained by replacing the Gaussian mixture noise with Gaussian noise with the same variance as shown in the next result.

Proposition 1: A closed-form achievable rate expression for secondary users in the presence of imperfect sensing decisions is given by

$$\begin{aligned} R_a &= \mathbb{E}_{g,h}\big\{R\big(P_0(g,h), P_1(g,h)\big)\big\} \\ &= \frac{T-\tau}{T} \sum_{k=0}^{1} \Pr(\hat{\mathcal{H}}_k) \mathbb{E}_{g,h}\left\{ \log_2\left(1 + \frac{P_k(g,h)|h|^2}{N_0 + \Pr(\mathcal{H}_1|\hat{\mathcal{H}}_k)\sigma_s^2}\right)\right\}, \end{aligned} \tag{8}$$

where $k \in \{0, 1\}$ and $\mathbb{E}\{.\}$ denotes expectation operation. Also, $\Pr\{\hat{\mathcal{H}}_1\}$ and $\Pr\{\hat{\mathcal{H}}_0\}$ denote the probabilities of channel being detected as busy and idle, respectively, and can be expressed as

$$\Pr\{\hat{\mathcal{H}}_1\} = \Pr\{\mathcal{H}_0\}\mathscr{P}_{\rm f} + \Pr\{\mathcal{H}_1\}\mathscr{P}_{\rm d}, \tag{9}$$

$$\Pr\{\hat{\mathcal{H}}_0\} = \Pr\{\mathcal{H}_0\}(1 - \mathscr{P}_{\rm f}) + \Pr\{\mathcal{H}_1\}(1 - \mathscr{P}_{\rm d}). \tag{10}$$

Proof: See Appendix A.

We note that since Gaussian is the worst-case noise [22], the achievable rate expression R_a in (8) is in general smaller than R_G in (7), which is the achievable rate obtained by considering the Gaussian-mixture noise. In the next result, we provide an upper bound on the difference between the two.

Theorem 1: The difference $(R_G - R_a)$ is upper bounded by (11), as shown at bottom of the next page where $c_1 = N_0 + \sigma_s^2$ and $c_2 = N_0$.

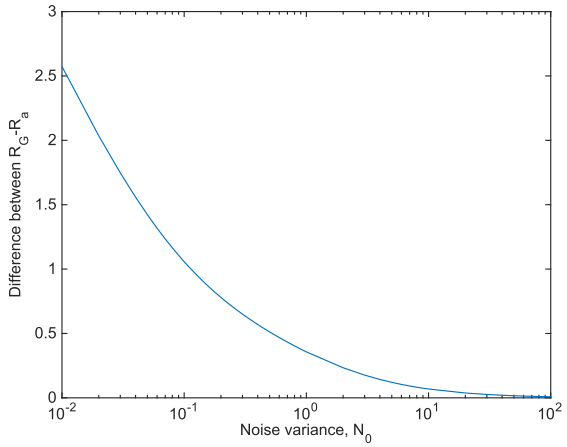

Fig. 2. Upper bound on the difference $(R_G - R_a)$ vs. noise variance N_0.

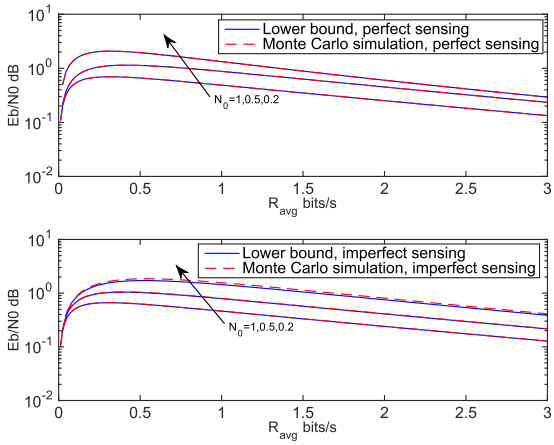

Fig. 3. Achievable EE η_{EE} vs. achievable rate R_a.

Proof: See Appendix B.

In Fig. 2, we plot the upper bound on the difference $(R_G - R_a)$ as a function of noise variance, N_0. We assume that $\mathscr{P}_{\text{d}} = 0.9$, $\mathscr{P}_{\text{f}} = 0.1$ and $\sigma_s^2 = 1$. It is seen that as noise variance, N_0, increases, the upper bound approaches zero, hence R_a, which can be regarded as a lower bound on the achievable rate R_G, becomes tighter.

With the characterization of the achievable rate in (8), we now define the EE as the ratio of the achievable rate to the total power consumption:

$$\eta_{\text{EE}} = \frac{\mathbb{E}_{g,h}\big\{R\big(P_0(g,h),\, P_1(g,h)\big)\big\}}{\mathbb{E}_{g,h}\{\Pr\{\hat{\mathcal{H}}_0\}P_0(g,h) + \Pr\{\hat{\mathcal{H}}_1\}P_1(g,h)\} + P_{\text{c}}}. \quad (12)$$

Above, the total power consists of average transmission power and circuit power, denoted by P_{c}. Circuit power represents the power consumed by the transmitter circuitry (i.e., by mixers, filters, and digital-to-analog converters, etc.), which is independent of transmission power.

The achievable EE expression in (12) can serve as a lower bound since the lower bound on achievable rate R_a in (8) is employed. The usefulness of this EE expression is due to its being an explicit function of the transmission power levels and sensing performance e.g., through the probabilities $\Pr\{\hat{\mathcal{H}}_0\}$, $\Pr\{\hat{\mathcal{H}}_1\}$, and $\Pr(\mathcal{H}_1|\hat{\mathcal{H}}_k)$.

In Fig. 3, we plot the EE expression in (12) (indicated as the lower bound) and the exact EE, in which we use Gaussian input and consider Gaussian mixture noise in the mutual information, as a function of achievable rate for both perfect sensing (i.e., $\mathscr{P}_{\text{d}} = 1$ and $\mathscr{P}_{\text{f}} = 0$) and imperfect sensing (i.e., $\mathscr{P}_{\text{d}} = 0.9$ and $\mathscr{P}_{\text{f}} = 0.2$). The graph is displayed in logarithmic scale to highlight the difference between the exact EE and the lower bound on EE. In order to evaluate the exact EE achieved with Gaussian input, we performed Monte Carlo simulations with 2×10^6 samples. In the case of perfect sensing, the lower bound and simulation result perfectly match as expected since in this case additive disturbance has Gaussian distribution rather than a Gaussian mixture. In the case of imperfect sensing, it is seen that the gap between the lower bound and exact EE decreases as N_0 increases, which matches with the characterization in Theorem 1. Additionally, since circuit power is taken into consideration with value $P_c = 0.1$W, EE vs. achievable rate curve is bell-shaped and is also quasiconcave. It is observed that maximum EE is achieved at nearly the same achievable rate for both lower bound and exact EE expressions.

In the following section, we derive power allocation schemes that maximize the EE of the secondary users in the presence of sensing errors, different combinations of transmit power and average interference power constraints, and different levels of CSI regarding the transmission and interference links.

III. Optimal Power Allocation

A. Average Transmit Power Constraint and Average Interference Power Constraint

In this subsection, we obtain the optimal power allocation strategies to maximize the EE of secondary users under average transmit power and average interference power constraints in the presence of different levels of CSI regarding the transmission and interference links, namely perfect CSI of both transmission and interference links, perfect CSI of the transmission link and imperfect CSI of the interference link, imperfect CSI of both links, or statistical CSI of both links.

$$R_G - R_a \le \left(\frac{T-\tau}{T}\right)\Bigg[\mathbb{E}_{g,h}\Bigg\{\sum_{k=1}^{2}\log_2\left(\frac{\sum_{i=1}^{2}\frac{\Pr(\mathcal{H}_i|\hat{\mathcal{H}}_k)}{c_i}}{\left(1+\frac{P_k(g,h)|h|^2}{N_0+\Pr(H_1|\hat{\mathcal{H}}_k)\sigma_s^2}\right)\sum_{i=1}^{2}\frac{\Pr(\mathcal{H}_i|\hat{\mathcal{H}}_k)}{c_i+|h|^2P_k(g,h)}}\right)\Bigg\}$$
$$-\sum_{k=1}^{2}\Pr(\hat{\mathcal{H}}_k)\left(\frac{N_0+\Pr(H_1|\hat{\mathcal{H}}_k)\sigma_s^2}{N_0+\sigma_s^2}\right)+\sum_{k=1}^{2}\Pr(\hat{\mathcal{H}}_k)\mathbb{E}_{g,h}\left\{1+\frac{\Pr(\mathcal{H}_1|\hat{\mathcal{H}}_k)\sigma_s^2}{N_0+|h|^2P_k(g,h)}\right\}\Bigg]. \quad (11)$$

1) Perfect CSI of Both Transmission and Interference Links: In this case, it is assumed that CSI of both transmission and interference links is perfectly known by the secondary transmitter. In this setting, the maximum EE under both average transmit power and interference power constraints can be found by solving the following optimization problem:

$$\max_{\substack{P_0(g,h)\\P_1(g,h)}} \eta_{\mathrm{EE}} = \frac{\mathbb{E}_{g,h}\left\{R\left(P_0(g,h),\, P_1(g,h)\right)\right\}}{\mathbb{E}_{g,h}\{\Pr\{\hat{\mathcal{H}}_0\}P_0(g,h)+\Pr\{\hat{\mathcal{H}}_1\}P_1(g,h)\}+P_{\mathrm{c}}} \tag{13}$$

subject to

$$\mathbb{E}_{g,h}\{\Pr\{\hat{\mathcal{H}}_0\}\, P_0(g,h) + \Pr\{\hat{\mathcal{H}}_1\}\, P_1(g,h)\} \le P_{\mathrm{avg}} \tag{14}$$

$$\mathbb{E}_{g,h}\{\left[(1-\mathscr{P}_{\mathrm{d}})\, P_0(g,h)+\mathscr{P}_{\mathrm{d}}\, P_1(g,h)\right]|g|^2\} \le Q_{\mathrm{avg}} \tag{15}$$

$$P_0(g,h) \ge 0,\, P_1(g,h) \ge 0, \tag{16}$$

where P_{avg} denotes the maximum average transmission power of the secondary transmitter and Q_{avg} represents the maximum allowed average interference power at the primary receiver. In particular, average transmit power constraint in (14) is chosen to satisfy the long-term power budget of the secondary users and average interference power constraint in (15) is imposed to limit the interference, and hence to protect the primary user transmission. In this setting, the optimal power allocation strategy that maximizes the EE of secondary users is determined in the following result.

Theorem 2: The optimal power allocation under the constraints in (14) and (15) is given by

$$P_0^*(g,h) = \left[\frac{\frac{T-\tau}{T}\Pr\{\hat{\mathcal{H}}_0\}\log_2 e}{(\lambda_1+\alpha)\Pr\{\hat{\mathcal{H}}_0\}+\nu_1|g|^2(1-\mathscr{P}_{\mathrm{d}})} - \frac{N_0+\Pr(\mathcal{H}_1|\hat{\mathcal{H}}_0)\sigma_s^2}{|h|^2}\right]^+ \tag{17}$$

$$P_1^*(g,h) = \left[\frac{\frac{T-\tau}{T}\Pr\{\hat{\mathcal{H}}_1\}\log_2 e}{(\lambda_1+\alpha)\Pr\{\hat{\mathcal{H}}_1\}+\nu_1|g|^2\mathscr{P}_{\mathrm{d}}} - \frac{N_0+\Pr(\mathcal{H}_1|\hat{\mathcal{H}}_1)\sigma_s^2}{|h|^2}\right]^+, \tag{18}$$

where $[x]^+$ *denotes* $\max(x,0)$*, α is a nonnegative parameter, and λ_1 and ν_1 are nonnegative Lagrange multipliers.*

Proof: See Appendix C.

Above, the Lagrange multipliers λ_1 and ν_1 can be jointly obtained by inserting the optimal power allocation schemes (17) and (18) into the constraints (14) and (15). However, solving these constraints does not give closed-form expressions for λ_1 and ν_1. Therefore, we employ the subgradient method, i.e., λ_1 and ν_1 are updated iteratively until convergence according to the subgradient direction in (19) and (20), shown at the bottom of this page, where n and t denote the iteration index and the step size, respectively. When the step size is chosen to be constant, it was shown that the subgradient method is guaranteed to converge to the optimal value within a small range [24].

Algorithm 1 Dinkelbach Method-Based Power Allocation That Maximizes EE of Cognitive Radio Systems Under Both Average Transmit Power and Interference Constraints

1: Initialization: $\mathscr{P}_{\mathrm{d}} = \mathscr{P}_{\mathrm{d,init}}$, $\mathscr{P}_{\mathrm{f}} = \mathscr{P}_{\mathrm{f,init}}$, $\epsilon > 0$, $\delta > 0$, $t > 0$, $\alpha^{(0)} = \alpha_{\mathrm{init}}$, $\lambda_1^{(0)} = \lambda_{1,\mathrm{init}}$, $\nu_1^{(0)} = \nu_{1,\mathrm{init}}$
2: $n \leftarrow 0$
3: **repeat**
4: calculate $P_0^*(g,h)$ and $P_1^*(g,h)$ using (17) and (18), respectively;
5: update λ_1 and ν_1 using subgradient method as follows:
6: $k \leftarrow 0$
7: **repeat**
8: $\lambda_1^{(k+1)} = \left[\lambda_1^{(k)} - t\big(P_{\mathrm{avg}} - \mathbb{E}_{g,h}\{\Pr\{\hat{\mathcal{H}}_0\}P_0^{(k)}(g,h) + \Pr\{\hat{\mathcal{H}}_1\}\, P_1^{(k)}(g,h)\}\big)\right]^+$
9: $\nu_1^{(k+1)} = \left[\nu_1^{(k)} - t\big(Q_{\mathrm{avg}} - \mathbb{E}_{g,h}\{[(1-\mathscr{P}_{\mathrm{d}})\, P_0^{(k)}(g,h)+ \mathscr{P}_{\mathrm{d}}P_1^{(k)}(g,h)]|g|^2\}\big)\right]^+$
10: $k \leftarrow k+1$
11: **until** $|\nu_1^{(k)}\big(Q_{\mathrm{avg}} - \mathbb{E}_{g,h}\{[(1-\mathscr{P}_{\mathrm{d}})\, P_0^{(k)}(g,h) + \mathscr{P}_{\mathrm{d}}P_1^{(k)}(g,h)]|g|^2\}\big)| \le \delta$ and $|\lambda_1^{(k)}\big(P_{\mathrm{avg}} - \mathbb{E}\{\Pr\{\hat{\mathcal{H}}_0\}\, P_0^{(k)}(g,h) + \Pr\{\hat{\mathcal{H}}_1\}\, P_1^{(k)}(g,h)\}\big)| \le \delta$
12: $\alpha^{(n+1)} = \frac{\mathbb{E}_{g,h}\left\{R\left(P_0^*(g,h),P_1^*(g,h)\right)\right\}}{\mathbb{E}_{g,h}\{\Pr\{\hat{\mathcal{H}}_0\}P_0^*(g,h)+\Pr\{\hat{\mathcal{H}}_1\}P_1^*(g,h)\}+P_{\mathrm{c}}}$
13: $n \leftarrow n+1$
14: **until** $|F(\alpha^{(n)})| \le \epsilon$

For a given value of α, the optimal power levels in (17), (18) can be found until $F(\alpha) \le \epsilon$ is satisfied. In the case of $F(\alpha) = 0$ in (102), the solution is optimal otherwise ϵ-optimal solution is obtained. In the following table, Dinkelbach method-based iterative power allocation algorithm for EE maximization under imperfect sensing is summarized. The proposed power control algorithm consists of two nested loops. In the outer loop, Dinkelbach's method iteratively solves the energy efficiency maximization problem by solving a sequence of parameterized concave problems. It is shown that Dinkelbach's method has a superlinear convergence rate [25], and hence the sequence converges to an optimal solution in a small number of iterations. In the inner loop, Lagrange multipliers are updated using the subgradient method, which involves the computation of subgradient and simple projection operations. The subgradient method is widely used to find Lagrange multipliers due to its simplicity, easy implementation, the speed for computing a direction, and the global convergence property [26]. Hence, the proposed algorithm is computationally efficient.

$$\lambda_1^{(n+1)} = \left[\lambda_1^{(n)} - t\big(P_{\mathrm{avg}} - \mathbb{E}_{g,h}\big\{\Pr\{\hat{\mathcal{H}}_0\}\, P_0^{(n)}(g,h) + \Pr\{\hat{\mathcal{H}}_1\}\, P_1^{(n)}(g,h)\big\}\big)\right]^+ \tag{19}$$

$$\nu_1^{(n+1)} = \left[\nu_1^{(n)} - t\big(Q_{\mathrm{avg}} - \mathbb{E}_{g,h}\{\left[(1-\mathscr{P}_{\mathrm{d}})\, P_0^{(n)}(g,h) + \mathscr{P}_{\mathrm{d}}\, P_1^{(n)}(g,h)\right]|g|^2\}\big)\right]^+ \tag{20}$$

Note that in the case of $\alpha = 0$, EE maximization problem is equivalent to maximizing the SE of the secondary user. Therefore, setting $\alpha = 0$ in (17) and (18) provides the optimal power allocation strategies that maximize the average achievable rate of secondary users.

Remark 1: The power allocation schemes in (17) and (18) have the structure of water-filling policy with respect to channel power gain $|h|^2$ between the secondary transmitter and secondary receiver, but average transmit and average interference power constraints are not necessarily satisfied with equality in constrast to to the case of throughput maximization. In addition, the water level in this policy depends on the interference channel power gain $|g|^2$ between the secondary transmitter and the primary receiver, i.e., less power is allocated when the interference link has a higher channel gain.

Remark 2: The proposed power allocation schemes in (17) and (18) depend on the sensing performance through detection and false alarm probabilities, $\mathscr{P}_{\rm d}$ and $\mathscr{P}_{\rm f}$, respectively. When both perfect sensing, i.e., $\mathscr{P}_{\rm d} = 1$ and $\mathscr{P}_{\rm f} = 0$, and SE maximization are considered, i.e., α is set to 0, the power allocation schemes become similar to that given in [27]. However, in our analysis the secondary users have two power allocation schemes depending on the presence or absence of active primary users.

2) Perfect CSI of Transmission Link and Imperfect CSI of Interference Link: In practice, it may be difficult to obtain perfect CSI of the interference link due to the lack of cooperation between secondary and primary users. In this case, the channel fading coefficient of the interference link can be expressed as [28]

$$g = \hat{g} + \tilde{g}, \tag{21}$$

where $\hat{g}$ denotes the estimate of the channel fading coefficient and $\tilde{g}$ represents the corresponding estimate error. It is assumed that $\hat{g}$ and $\tilde{g}$ follow independent, circularly symmetric complex Gaussian distributions with mean zero and variances $1-\sigma_g^2$ and σ_g^2, respectively, i.e., $\hat{g} \sim \mathcal{N}(0, 1-\sigma_g^2)$ and $\tilde{g} \sim \mathcal{N}(0, \sigma_g^2)$. Another formulation for modeling the imperfect CSI is given by [29] via the correlation coefficient, where the estimate and the corresponding estimation error of the channel fading coefficient follow the same distribution as in (21). Under this assumption, the average interference constraint can be written as

$$\begin{aligned} Q_{\rm avg} &\geq \mathbb{E}_{g,\hat{g},h}\{\big[(1-\mathscr{P}_{\rm d})P_0(\hat{g},h) + \mathscr{P}_{\rm d}P_1(\hat{g},h)\big]|g|^2\} \\ &= \mathbb{E}_{\hat{g},h}\{\big[(1-\mathscr{P}_{\rm d})P_0(\hat{g},h) + \mathscr{P}_{\rm d}P_1(\hat{g},h)\big](|\hat{g}|^2+|\tilde{g}|^2)\} \\ &= \mathbb{E}_{\hat{g},h}\{\big[(1-\mathscr{P}_{\rm d})P_0(\hat{g},h) + \mathscr{P}_{\rm d}P_1(\hat{g},h)\big](|\hat{g}|^2+\sigma_g^2)\}, \end{aligned} \tag{22}$$

where the power levels P_0 and P_1 are now expressed as functions of the estimate $\hat{g}$. Now, the optimal power allocation problem under the assumptions of perfect instantaneous CSI of the transmission link and imperfect instantaneous CSI of the interfence link can be formulated as follows:

$$\max_{\substack{P_0(\hat{g},h)\\P_1(\hat{g},h)}} \eta_{\rm EE} = \frac{\mathbb{E}_{\hat{g},h}\big\{R\big(P_0(\hat{g},h),P_1(\hat{g},h)\big)\big\}}{\mathbb{E}_{\hat{g},h}\{\Pr\{\hat{\mathcal{H}}_0\}P_0(\hat{g},h)+\Pr\{\hat{\mathcal{H}}_1\}P_1(\hat{g},h)\}+P_{\rm c}} \tag{23}$$

subject to

$$\mathbb{E}_{\hat{g},h}\{\Pr\{\hat{\mathcal{H}}_0\}\,P_0(\hat{g},h) + \Pr\{\hat{\mathcal{H}}_1\}\,P_1(\hat{g},h)\} \leq P_{\rm avg} \tag{24}$$

$$\mathbb{E}_{\hat{g},h}\{\big[(1-\mathscr{P}_{\rm d})\,P_0(\hat{g},h) + \mathscr{P}_{\rm d}\,P_1(\hat{g},h)\big](|\hat{g}|^2+\sigma_g^2)\} \leq Q_{\rm avg}$$
$$P_0(\hat{g},h) \geq 0,\, P_1(\hat{g},h) \geq 0 \tag{25}$$

In the following result, we determine the optimal power allocation strategy in closed-form for this case.

Theorem 3: The optimal power allocation subject to the constraints in (24) and (25) is obtained as (27) and (28), shown at the bottom of this page, where λ_2 and ν_2 are nonnegative Lagrange multipliers associated with the average transmit power in (24) and average interference power constraints in (25), respectively.

Proof: We mainly follow the same steps as in the proof of Theorem 2, but with several modifications due to imperfect knowledge of the interference link. More specifically, the KKT conditions now become

$$\frac{\frac{T-\tau}{T}\Pr\{\hat{\mathcal{H}}_0\}|h|^2\log_2 e}{N_0+\Pr(\mathcal{H}_1|\hat{\mathcal{H}}_0)\sigma_s^2+P_0^*(\hat{g},h)|h|^2} - (\lambda_2+\alpha)\Pr\{\hat{\mathcal{H}}_0\} - \nu_2(|\hat{g}|^2+\sigma_g^2)(1-\mathscr{P}_{\rm d}) = 0 \tag{29}$$

$$\frac{\frac{T-\tau}{T}\Pr\{\hat{\mathcal{H}}_1\}|h|^2\log_2 e}{N_0+\Pr(\mathcal{H}_1|\hat{\mathcal{H}}_1)\sigma_s^2+P_1^*(g,h)|h|^2} - (\lambda_2+\alpha)\Pr\{\hat{\mathcal{H}}_1\} - \nu_2(|\hat{g}|^2+\sigma_g^2)\mathscr{P}_{\rm d} = 0 \tag{30}$$

$$\lambda_2\Big(\mathbb{E}_{\hat{g},h}\Big\{\Pr\{\hat{\mathcal{H}}_0\}\,P_0^*(\hat{g},h) + \Pr\{\hat{\mathcal{H}}_1\}\,P_1^*(\hat{g},h)\Big\} - P_{\rm avg}\Big) = 0 \tag{31}$$

$$\nu_2\Big(\mathbb{E}_{\hat{g},h}\Big\{\big[(1-\mathscr{P}_{\rm d})\,P_0^*(\hat{g},h) + \mathscr{P}_{\rm d}\,P_1^*(\hat{g},h)\big](|\hat{g}|^2+\sigma_g^2)\Big\} - Q_{\rm avg}\Big) = 0 \tag{32}$$

$$\lambda_2 \geq 0, \quad \nu_2 \geq 0. \tag{33}$$

Solving for $P_0^*(\hat{g},h)$ in (29) and $P_1^*(\hat{g},h)$ in (30) lead to the optimal power values in (27) and (28), as shown at the bottom this page respectively. □

Remark 3: We note that the optimal power levels in (27) and (28) now depend on the channel estimation error of the

$$P_0^*(\hat{g},h) = \left[\frac{\frac{T-\tau}{T}\Pr\{\hat{\mathcal{H}}_0\}\log_2 e}{(\lambda_2+\alpha)\Pr\{\hat{\mathcal{H}}_0\}+\nu_2(1-\mathscr{P}_{\rm d})(|\hat{g}|^2+\sigma_g^2)} - \frac{N_0+\Pr(\mathcal{H}_1|\hat{\mathcal{H}}_0)\sigma_s^2}{|h|^2}\right]^+ \tag{27}$$

$$P_1^*(\hat{g},h) = \left[\frac{\frac{T-\tau}{T}\Pr\{\hat{\mathcal{H}}_1\}\log_2 e}{(\lambda_2+\alpha)\Pr\{\hat{\mathcal{H}}_1\}+\nu_2\mathscr{P}_{\rm d}(|\hat{g}|^2+\sigma_g^2)} - \frac{N_0+\Pr(\mathcal{H}_1|\hat{\mathcal{H}}_1)\sigma_s^2}{|h|^2}\right]^+, \tag{28}$$

interference link, σ_g^2. More specifically, the water level is also determined by σ_g^2, i.e., inaccurate estimation with higher channel estimation error results in lower water levels, hence lower transmission powers.

Remark 4: We can readily obtain the power allocation schemes under perfect sensing by setting $\mathscr{P}_{\rm d}=1$ and $\mathscr{P}_{\rm f}=0$ in (27) and (28). In addition, the proposed power schemes capture the power levels under perfect CSI of the interference link as a special case when $\sigma_g^2=0$.

3) Imperfect CSI of Both Transmission and Interference Links: In this case, we assume that in addition to the imperfect knowledge of the interference link, the secondary transmitter has imperfect CSI of the transmission link. The channel fading coefficient of the transmission link is written as

$$h=\hat{h}+\tilde{h}. \tag{34}$$

Above, $\hat{h}$ is the estimate of the channel fading coefficient of the transmission link and $\tilde{h}$ is the corresponding estimation error. It is assumed that $\hat{h}$ and $\tilde{h}$ are independent, circularly symmetric complex Gaussian distributed with zero mean and variances $1-\sigma_h^2$ and σ_h^2, respectively, i.e., $\hat{h}\sim\mathcal{N}(0,1-\sigma_h^2)$ and $\tilde{h}\sim\mathcal{N}(0,\sigma_h^2)$. In this case, by taking into account imperfect CSI of both links, the achievable rate of secondary users is given by

$$\begin{aligned}R_a &= \mathbb{E}_{\hat{g},\hat{h},h}\big\{R\big(P_0(\hat{g},\hat{h}),P_1(\hat{g},\hat{h})\big)\big\}\\ &= \frac{T-\tau}{T}\sum_{k=0}^{1}\Pr(\hat{\mathcal{H}}_k)\int_{\hat{g}}\\ &\quad\times\left(\int_{\hat{h}}\left(\int_{|h|^2}\log_2\left(1+\frac{P_k(\eta,\zeta)\gamma}{N_0+\Pr(\mathcal{H}_1|\hat{\mathcal{H}}_k)\sigma_s^2}\right)\right.\right.\\ &\quad\left.\left.\times f_{|h|^2|\hat{h}}(\gamma\mid\hat{h})d\gamma\right)f_{\hat{h}}(\zeta)d\zeta\right)f_{\hat{g}}(\eta)d\eta,\end{aligned} \tag{35}$$

where $f_{|h|^2|\hat{h}}(\gamma\mid\hat{h})$ denotes the probability density function (pdf) of $|h|^2$ conditioned on $\hat{h}$, and in the case of Rayleigh fading, the corresponding pdf is given by

$$f_{|h|^2|\hat{h}}(\gamma\mid\hat{h})=\frac{1}{\alpha_h^2}\mathrm{e}^{-\frac{\gamma+|\hat{h}|^2}{\alpha_h^2}}I_0\left(\frac{2}{\alpha_h^2}\sqrt{|\hat{h}|^2\gamma}\right), \tag{36}$$

where $I_0(.)$ represents the modified Bessel function of the first kind [30]. Consequently, the optimal power allocation problem can be expressed as

$$\max_{\substack{P_0(\hat{g},\hat{h})\\P_1(\hat{g},\hat{h})}}\ \eta_{\rm EE}=\frac{\mathbb{E}_{\hat{g},\hat{h},h}\big\{R\big(P_0(\hat{g},\hat{h}),P_1(\hat{g},\hat{h})\big)\big\}}{\mathbb{E}_{\hat{g},\hat{h},h}\{\Pr\{\hat{\mathcal{H}}_0\}P_0(\hat{g},\hat{h})+\Pr\{\hat{\mathcal{H}}_1\}P_1(\hat{g},\hat{h})\}+P_{\rm c}} \tag{37}$$

subject to

$$\mathbb{E}_{\hat{g},\hat{h},h}\{\Pr\{\hat{\mathcal{H}}_0\}\,P_0(\hat{g},\hat{h})+\Pr\{\hat{\mathcal{H}}_1\}\,P_1(\hat{g},\hat{h})\}\le P_{\rm avg} \tag{38}$$

$$\mathbb{E}_{\hat{g},\hat{h},h}\{\big[(1-\mathscr{P}_{\rm d})P_0(\hat{g},\hat{h})+\mathscr{P}_{\rm d}P_1(\hat{g},\hat{h})\big](|\hat{g}|^2+\sigma_g^2)\}\le Q_{\rm avg} \tag{39}$$

$$P_0(\hat{g},\hat{h})\ge 0,\quad P_1(\hat{g},\hat{h})\ge 0 \tag{40}$$

We obtain the following result for the optimal power allocation scheme.

Theorem 4: The optimal power allocation subject to the constraints in (38) and (39) is obtained as

$$P_0^*(\hat{g},\hat{h})=\bar{P}_0(\hat{g},\hat{h}) \tag{41}$$

$$P_1^*(\hat{g},\hat{h})=\bar{P}_1(\hat{g},\hat{h}), \tag{42}$$

where $\bar{P}_0(\hat{g},\hat{h})$ and $\bar{P}_1(\hat{g},\hat{h})$ are the solutions, respectively, to the following equations

$$\begin{aligned}&\int_0^\infty\frac{\left(\frac{T-\tau}{T}\right)\Pr\{\hat{\mathcal{H}}_0\}\log_2 e\gamma}{N_0+\Pr\{\hat{\mathcal{H}}_0\}\sigma_s^2+\bar{P}_0(\hat{g},\hat{h})\gamma}f_{|h|^2|\hat{h}}(\gamma,\hat{h})d\gamma\\ &\quad=(\lambda_3+\alpha)\Pr\{\hat{\mathcal{H}}_0\}+\nu_3(1-\mathscr{P}_{\rm d})(|\hat{g}|^2+\sigma_g^2)\end{aligned} \tag{43}$$

$$\begin{aligned}&\int_0^\infty\frac{\left(\frac{T-\tau}{T}\right)\Pr\{\hat{\mathcal{H}}_1\}\log_2 e\gamma}{N_0+\Pr\{\hat{\mathcal{H}}_1\}\sigma_s^2+\bar{P}_1(\hat{g},\hat{h})\gamma}f_{|h|^2|\hat{h}}(\gamma,\hat{h})d\gamma\\ &\quad=(\lambda_3+\alpha)\Pr\{\hat{\mathcal{H}}_1\}+\nu_3\mathscr{P}_{\rm d}(|\hat{g}|^2+\sigma_g^2).\end{aligned} \tag{44}$$

If there are no positive solutions for (43) and (44) given the values of $\hat{g}$ and $\hat{h}$, the instantaneous power levels are set to zero, i.e., $P_0^*(\hat{g},\hat{h})=0$ and $P_1^*(\hat{g},\hat{h})=0$.

Proof: Similar to the proof of Theorem 2, we first express the optimization problem in a subtractive form, which is a concave function of transmission power levels, and then define the Lagrangian as

$$\begin{aligned}&L(P_0,P_1,\lambda_3,\nu_3,\alpha)\\ &=\mathbb{E}_{\hat{g},\hat{h},h}\big\{R\big(P_0(\hat{g},\hat{h}),P_1(\hat{g},\hat{h})\big)\big\}\\ &\quad-\alpha(\mathbb{E}_{\hat{g},\hat{h},h}\{\Pr\{\hat{\mathcal{H}}_0\}P_0(\hat{g},\hat{h})+\Pr\{\hat{\mathcal{H}}_1\}P_1(\hat{g},\hat{h})\}+P_{\rm c})\\ &\quad-\lambda_3(\mathbb{E}_{\hat{g},\hat{h},h}\{\Pr\{\hat{\mathcal{H}}_0\}\,P_0(\hat{g},\hat{h})+\Pr\{\hat{\mathcal{H}}_1\}\,P_1(\hat{g},\hat{h})\}-P_{\rm avg})\\ &\quad-\nu_3(\mathbb{E}_{\hat{g},\hat{h},h}\{\big[(1-\mathscr{P}_{\rm d})\,P_0(\hat{g},\hat{h})+\mathscr{P}_{\rm d}\,P_1(\hat{g},\hat{h})\big](|\hat{g}|^2+\sigma_g^2)\}\\ &\qquad-Q_{\rm avg}).\end{aligned} \tag{45}$$

Setting the derivatives of the Lagrangian in (45) with respect to $P_0^*(\hat{g},\hat{h})$ and $P_1^*(\hat{g},\hat{h})$ to zero and arranging the terms yield the desired results in (43) and (44), respectively. □ □

Remark 5: Let $f_0(P_0(\hat{g},\hat{h}))$ and $f_1(P_1(\hat{g},\hat{h}))$ denote the left-hand sides of (43) and (44), respectively, as a function of the transmission powers and let ω_0 and ω_1 denote the right-hand sides of (43) and (44), respectively. For given values of $\hat{g}$ and $\hat{h}$, $f_0(P_0(\hat{g},\hat{h}))$ and $f_1(P_1(\hat{g},\hat{h}))$ are positive decreasing functions of transmission powers with their maximum values $f_0(0)$ and $f_1(0)$ obtained at $P_0(\hat{g},\hat{h})=0$ and $P_1(\hat{g},\hat{h})=0$, respectively. Hence, the optimal solutions P_0^* and P_1^* can be characterized as

$$P_0^*=\begin{cases}f_0^{-1}(\omega_0) & 0<\omega_0<f_0(0)\\ 0 & \omega_0\ge f_0(0)\end{cases} \tag{46}$$

$$P_1^*=\begin{cases}f_1^{-1}(\omega_1) & 0<\omega_1<f_1(0)\\ 0 & \omega_1\ge f_1(0).\end{cases} \tag{47}$$

It is seen from the above expressions that we allocate power only when $f_0(0)>\omega_0$ and $f_1(0)>\omega_1$, otherwise power levels are zero. Also, the average transmission powers attained with the proposed above optimal power levels are decreasing functions of ω_1 and ω_2, respectively since $f_0^{-1}(\omega_0)$ and $f_1^{-1}(\omega_1)$ are decreasing in ω_0 and ω_1, respectively. Hence,

in that sense, the optimal power allocation can be interpreted again as water-filling policy.

Remark 6: The proposed power levels in (41) and (42) are functions of the variance of the estimation error of the transmission link, σ_h^2 and interference link, σ_g^2. Hence, Theorem 4 can be seen as a generalization of the power allocation schemes attained under perfect CSI of transmission link and interference links, i.e., this case can be recovered by setting $\sigma_h^2 = 0$ and $\sigma_g^2 = 0$.

4) Statistical CSI of Both Transmission and interference Links: In this case, the secondary transmitter has only statistical CSI of both transmission and interference links, i.e., knows only the fading distribution of both transmission and interference links. Under this assumption, the power allocation problem is formulated as follows:

$$\max_{P_0,P_1} \eta_{\mathrm{EE}} = \frac{R(P_0,P_1)}{\mathbb{E}\{\Pr\{\hat{\mathcal{H}}_0\}P_0+\Pr\{\hat{\mathcal{H}}_1\}P_1\}+P_{\mathrm{c}}} \tag{48}$$

$$\text{subject to } \mathbb{E}\{\Pr\{\hat{\mathcal{H}}_0\}\,P_0+\Pr\{\hat{\mathcal{H}}_1\}\,P_1\} \le P_{\mathrm{avg}} \tag{49}$$

$$\mathbb{E}\{\left[(1-\mathscr{P}_{\mathrm{d}})\,P_0+\mathscr{P}_{\mathrm{d}}\,P_1\right]|g|^2\} \le Q_{\mathrm{avg}} \tag{50}$$

$$P_0 \ge 0, \quad P_1 \ge 0 \tag{51}$$

Note that transmission power levels P_0 and P_1 are no longer functions of g and h. There are no closed-form expressions for the optimal power levels P_0^* and P_1^*. However, we can solve (48) numerically by transforming the optimization problem into an equivalent parametrized concave form and using convex optimization tools.

B. Peak Transmit Power Constraint and Average Interference Power Constraint

In this section, we assume that peak transmit power constraints are imposed rather than average power constraints. Interference is still controlled via average interference constraints. Peak transmit power constraint is imposed to limit the instantaneous transmit power of the secondary users, and hence corresponds to a stricter constraint compared to the average transmit power constraint.

1) Perfect CSI of Both Transmission and Interference Links: Energy-efficient power allocation under the assumption of perfect CSI of both transmission and interference links can be obtained by solving the following problem:

$$\max_{\substack{P_0(g,h)\\P_1(g,h)}} \eta_{\mathrm{EE}} = \frac{\mathbb{E}_{g,h}\{R(P_0(g,h),P_1(g,h))\}}{\mathbb{E}_{g,h}\{\Pr\{\hat{\mathcal{H}}_0\}P_0(g,h)+\Pr\{\hat{\mathcal{H}}_1\}P_1(g,h)\}+P_{\mathrm{c}}} \tag{52}$$

subject to

$$P_0(g,h) \le P_{\mathrm{pk},0} \tag{53}$$

$$P_1(g,h) \le P_{\mathrm{pk},1} \tag{54}$$

$$\mathbb{E}_{g,h}\{\left[(1-\mathscr{P}_{\mathrm{d}})\,P_0(g,h)+\mathscr{P}_{\mathrm{d}}\,P_1(g,h)\right]|g|^2\} \le Q_{\mathrm{avg}} \tag{55}$$

$$P_0(g,h) \ge 0, \quad P_1(g,h) \ge 0, \tag{56}$$

where $P_{\mathrm{pk},0}$ and $P_{\mathrm{pk},1}$ denote the peak transmit power limits when the channel is detected as idle and busy, respectively. Under the above constraints, the optimal power allocation strategy is determined in the following result.

Theorem 5: The optimal power allocation scheme that maximizes the EE of the secondary users subject to the constraints in (53), (54) and (55) is given by (57) and (58), shown at the bottom of this page, where

$$\breve{g}_{1,j} = \frac{1}{\nu_4\rho_j}\left(\frac{\frac{T-\tau}{T}\Pr\{\hat{\mathcal{H}}_j\}\log_2 e|h|^2}{N_0+\Pr(\mathcal{H}_1|\hat{\mathcal{H}}_j)\sigma_s^2}-\alpha\Pr\{\hat{\mathcal{H}}_j\}\right), \tag{59}$$

$$\breve{g}_{2,j} = \frac{1}{\nu_4\rho_j}\left(\frac{\frac{T-\tau}{T}\Pr\{\hat{\mathcal{H}}_j\}\log_2 e|h|^2}{P_{pk,j}|h|^2+N_0+\Pr(\mathcal{H}_1|\hat{\mathcal{H}}_j)\sigma_s^2}-\alpha\Pr\{\hat{\mathcal{H}}_j\}\right). \tag{60}$$

In the above expressions, $j \in \{0,1\}$, $\rho_0 = 1-\mathscr{P}_{\mathrm{d}}$ and $\rho_1 = \mathscr{P}_{\mathrm{d}}$.

Proof: By transforming the above optimization problem into an equivalent parametrized concave form and following the same steps as in the proof of Theorem 2 with peak transmit power constraints instead of average transmit power constraint, we can readily obtain the optimal power allocation schemes as in (57) and (58), respectively. □

Remark 7: Different from Theorem 2, the optimal power levels are limited by $P_{pk,0}$ and $P_{pk,1}$, respectively, when the channel fading coefficient of the interference link is less than a certain threshold, which is mainly determined by the sensing performance through the detection and false-alarm probabilities.

$$P_0^*(g,h) = \begin{cases} 0, & |g|^2 \ge \breve{g}_{1,0} \\ \dfrac{\frac{T-\tau}{T}\Pr\{\hat{\mathcal{H}}_0\}\log_2 e}{\nu_4|g|^2(1-\mathscr{P}_{\mathrm{d}})+\alpha\Pr\{\hat{\mathcal{H}}_0\}} - \dfrac{N_0+\Pr(\mathcal{H}_1|\hat{\mathcal{H}}_0)\sigma_s^2}{|h|^2}, & \breve{g}_{1,0} > |g|^2 > \breve{g}_{2,0} \\ P_{\mathrm{pk},0}, & |g|^2 \le \breve{g}_{2,0} \end{cases} \tag{57}$$

$$P_1^*(g,h) = \begin{cases} 0, & |g|^2 \ge \breve{g}_{1,1} \\ \dfrac{\frac{T-\tau}{T}\Pr\{\hat{\mathcal{H}}_1\}\log_2 e}{\nu_4|g|^2\mathscr{P}_{\mathrm{d}}+\alpha\Pr\{\hat{\mathcal{H}}_1\}} - \dfrac{N_0+\Pr(\mathcal{H}_1|\hat{\mathcal{H}}_1)\sigma_s^2}{|h|^2}, & \breve{g}_{1,1} > |g|^2 > \breve{g}_{2,1} \\ P_{\mathrm{pk},1}, & |g|^2 \le \breve{g}_{2,1} \end{cases} \tag{58}$$

Remark 8: By setting $\alpha = 0$, $\mathscr{P}_{\rm d} = 1$ and $\mathscr{P}_{\rm f} = 0$ in (57) and (58), we can see that the power allocation schemes in (57) and (58) have similar structures as those in [27] in the case of throughput maximization where average interference power constraint is satisfied with equality. However, this constraint is not necessarily satistifed with equality in EE maximization.

Algorithm 1 can be modified to maximize the EE subject to peak power constraints and average interference constraint in such a way that $P_0^*(g,h)$ and $P_1^*(g,h)$ are computed using (57) and (58), respectively and only Lagrange multiplier ν_4 is updated according to (20).

2) Perfect CSI of the Transmission Link and Imperfect CSI of the Interference Link: In the presence of perfect CSI of the transmission link and imperfect CSI of the interference link, the optimization problem in (23) is subject to

$$P_0(\hat{g},h) \le P_{\rm pk,0} \tag{61}$$

$$P_1(\hat{g},h) \le P_{\rm pk,1} \tag{62}$$

$$\mathbb{E}_{\hat{g},h}\{\left[(1-\mathscr{P}_{\rm d})\,P_0(\hat{g},h)+\mathscr{P}_{\rm d}\,P_1(\hat{g},h)\right](|\hat{g}|^2+\sigma_g^2)\} \le Q_{\rm avg} \tag{63}$$

In this setting, the optimal power levels, $P_0^*(\hat{g},h)$ and $P_1^*(\hat{g},h)$ are obtained by setting $\lambda_2 = 0$ in (27) and (28), and incorporating the peak power constraints in (61) and (62) to limit the power levels by $P_{\rm pk,0}$ and $P_{\rm pk,1}$, respectively.

Remark 9: As different from the results in Theorem 5, the cut-off values in the optimal power allocation schemes subject to the constrains in (61), (62) and (63) depend on the channel estimation error variance of the interference link.

3) Imperfect CSI of Both Transmission and Interference Links: We again have peak transmit power and average interference power constraints. However, different from the previous subsections, the transmission link is imperfectly known at the secondary transmitter. Therefore, the power levels are functions of $\hat{g}$ and $\hat{h}$. In this case, the optimal power allocation scheme that maximizes the EE of the secondary users can be found by setting the Lagrange multiplier, λ_3 in (43) and (44) equal to zero and limiting the instantaneous power levels by $P_{\rm pk,0}$ and $P_{\rm pk,1}$, respectively.

4) Statistical CSI of Both Transmission and Interference Links: In this case, the optimal power allocation problem is subject to peak transmit and average interference power constraints under the assumption of the availability of only statistical CSI of both transmission and interference links. The optimal values of P_0^* and P_1^* can be found numerically by converting the optimization problem into an equivalent parametrized concave form and employing convex optimization tools.

C. Average Transmit Power Constraint and Peak Interference Power Constraint

Finally, we consider the case in which the secondary transmitter operates under average transmit power constraint and peak interference power constraints, which are imposed to satisfy short-term QoS requirements of the primary users.

1) Perfect CSI of Both Transmission and Interference Links: In this case, the objective function in (13) is subject to the following constraints:

$$\mathbb{E}_{g,h}\{\Pr\{\hat{\mathcal{H}}_0\}\,P_0(g,h)+\Pr\{\hat{\mathcal{H}}_1\}\,P_1(g,h)\} \le P_{\rm avg} \tag{64}$$

$$P_0(g,h)|g|^2 \le Q_{\rm pk,0} \tag{65}$$

$$P_1(g,h)|g|^2 \le Q_{\rm pk,1} \tag{66}$$

where $Q_{{\rm pk},k}$ for $k \in \{0,1\}$ represents the peak limit on the received interference power at the primary receiver. Under these constraints, we derive the optimal power allocation scheme as follows:

Theorem 6: The optimal power allocation strategy under average transmit power in (64) and peak interference power constraints in (65) and (66) is obtained as

$$P_0^*(g,h) = \min\left(\left[\frac{\frac{T-\tau}{T}\log_2 e}{(\lambda_4+\alpha)} - \frac{N_0+\Pr(\mathcal{H}_1|\hat{\mathcal{H}}_0)\sigma_s^2}{|h|^2}\right]^+, \frac{Q_{pk,0}}{|g|^2}\right) \tag{67}$$

$$P_1^*(g,h) = \min\left(\left[\frac{\frac{T-\tau}{T}\log_2 e}{(\lambda_4+\alpha)} - \frac{N_0+\Pr(\mathcal{H}_1|\hat{\mathcal{H}}_1)\sigma_s^2}{|h|^2}\right]^+, \frac{Q_{pk,1}}{|g|^2}\right) \tag{68}$$

Above, λ_4 is the Lagrange multiplier associated with the average transmit power in (64).

Proof: The optimization problem is first expressed in terms of an equivalent concave form. Then, the similar steps as in the proof of Theorem 2 are followed. However, peak interference power constraints are imposed instead of average interference power constraint. Therefore, in this case the optimal powers are limited by peak interference power constraints, $Q_{{\rm pk},k}$ for $k \in \{0,1\}$. □

2) Perfect CSI of the Transmission Link and Imperfect CSI of the Interference Link: We have the following constraints for the optimization problem in (23):

$$\mathbb{E}_{g,h}\{\Pr\{\hat{\mathcal{H}}_0\}\,P_0(\hat{g},h)+\Pr\{\hat{\mathcal{H}}_1\}\,P_1(\hat{g},h)\} \le P_{\rm avg} \tag{69}$$

$$\Pr(P_0(\hat{g},h)|g|^2 \ge Q_{\rm pk,0}|\hat{g}) \le \xi_0 \tag{70}$$

$$\Pr(P_1(\hat{g},h)|g|^2 \ge Q_{\rm pk,1}|\hat{g}) \le \xi_1 \tag{71}$$

where ξ_k for $k \in \{0,1\}$ denotes the outage threshold. Note that if the interference link CSI is imperfect, peak interference limit cannot be always satisfied and hence the peak interference constraints are modified as peak interference outage constraints. The constraints in (70) and (71) can be further expressed as [31]

$$P_0(\hat{g},h) \le \frac{Q_{\rm pk,0}}{F^{-1}_{|g|^2|\hat{g}}(1-\xi_0,\hat{g})} \tag{72}$$

$$P_1(\hat{g},h) \le \frac{Q_{\rm pk,1}}{F^{-1}_{|g|^2|\hat{g}}(1-\xi_1,\hat{g})}. \tag{73}$$

Above, $F^{-1}_{|g|^2|\hat{g}}(.,\hat{g})$ represents the inverse cumulative density function of $|g|^2$ given $\hat{g}$. In this setting, the main characterization is given as follows:

Theorem 7: The optimal power allocation strategy under the constraints in (69), (70) and (71) is given by

$$P_0^*(\hat{g},h) = \min\left(\left[\frac{\frac{T-\tau}{T}\log_2 e}{(\lambda_5+\alpha)} - \frac{N_0+\Pr(\mathcal{H}_1|\hat{\mathcal{H}}_0)\sigma_s^2}{|h|^2}\right]^+, \frac{Q_{pk,0}}{F^{-1}_{|g|^2|\hat{g}}(1-\xi_0,\hat{g})}\right) \quad (74)$$

$$P_1^*(\hat{g},h) = \min\left(\left[\frac{\frac{T-\tau}{T}\log_2 e}{(\lambda_5+\alpha)} - \frac{N_0+\Pr(\mathcal{H}_1|\hat{\mathcal{H}}_1)\sigma_s^2}{|h|^2}\right]^+, \frac{Q_{pk,1}}{F^{-1}_{|g|^2|\hat{g}}(1-\xi_1,\hat{g})}\right) \quad (75)$$

Above, λ_5 is the Lagrange multiplier.

Proof: The optimization problem in (23) is first expressed in terms of the equivalent parameterized form as in (98). Then, the Lagrangian is written as follows

$$\begin{aligned} &L(P_0,P_1,\lambda_5,\alpha)\\ &= \mathbb{E}_{\hat{g},h}\big\{R\big(P_0(\hat{g},h),P_1(\hat{g},h)\big)\big\}\\ &\quad - \alpha\Big(\mathbb{E}_{\hat{g},h}\{\Pr\{\hat{\mathcal{H}}_0\}P_0(\hat{g},h)+\Pr\{\hat{\mathcal{H}}_1\}P_1(\hat{g},h)\}+P_{\rm c}\Big)\\ &\quad - \lambda_5\Big(\mathbb{E}_{\hat{g},h}\{\Pr\{\hat{\mathcal{H}}_0\}\,P_0(\hat{g},h)+\Pr\{\hat{\mathcal{H}}_1\}\,P_1(\hat{g},h)\}-P_{\rm avg}\Big). \end{aligned} \quad (76)$$

By setting the derivative of the above function with respect to $P_0(\hat{g},h)$ and $P_1(\hat{g},h)$ equal to zero at the optimal power levels, respectively, solving the resulting equations in terms of $P_0^*(\hat{g},h)$ and $P_1^*(\hat{g},h)$, and incorporating the peak interference power constraints in (72) and (73), lead to the desired results in (74) and (75), respectively. □

Remark 10: The optimal power allocation scheme is limited by $\frac{Q_{pk,k}}{F^{-1}_{|g|^2|\hat{g}}(1-\xi_k,\hat{g})}$ for $k\in\{0,1\}$, which depends on the outage threshold and the channel estimate of the interference link. As the allowed interference outage level is increased, the secondary users can transmit with higher power levels.

3) Imperfect CSI of Both Transmission and Interference Links: It is assumed that the secondary users operate under the constraints below:

$$\mathbb{E}_{\hat{g},\hat{h},h}\{\Pr\{\hat{\mathcal{H}}_0\}\,P_0(\hat{g},\hat{h})+\Pr\{\hat{\mathcal{H}}_1\}\,P_1(\hat{g},\hat{h})\}\le P_{\rm avg} \quad (77)$$

$$P_0(\hat{g},\hat{h}) \le \frac{Q_{\rm pk,0}}{F^{-1}_{|g|^2|\hat{g}}(1-\xi_0,\hat{g})} \quad (78)$$

$$P_1(\hat{g},\hat{h}) \le \frac{Q_{\rm pk,1}}{F^{-1}_{|g|^2|\hat{g}}(1-\xi_1,\hat{g})}. \quad (79)$$

In the following result, we derive the optimal power allocation scheme for this case.

Theorem 8: The optimal power allocation strategy under average transmit power in (77) and peak interference power constraints in (78) and (79) is obtained as

$$P_0^*(\hat{g},\hat{h}) = \min\left(\frac{Q_{pk,0}}{F^{-1}_{|g|^2|\hat{g}}(1-\xi_0,\hat{g})},\bar{P}_0(\hat{g},\hat{h})\right), \quad (80)$$

$$P_1^*(\hat{g},\hat{h}) = \min\left(\frac{Q_{pk,1}}{F^{-1}_{|g|^2|\hat{g}}(1-\xi_1,\hat{g})},\bar{P}_1(\hat{g},\hat{h})\right) \quad (81)$$

where $\bar{P}_0(\hat{g},\hat{h})$ is solution to

$$\int_0^\infty \frac{\left(\frac{T-\tau}{T}\right)\Pr\{\hat{\mathcal{H}}_0\}\log_2 e\gamma}{N_0+\Pr\{\hat{\mathcal{H}}_0\}\sigma_s^2+\bar{P}_0(\hat{g},\hat{h})\gamma} f_{|h|^2|\hat{h}}(\gamma,\hat{h})d\gamma = (\lambda_6+\alpha)\Pr\{\hat{\mathcal{H}}_0\} \quad (82)$$

and $\bar{P}_1(\hat{g},\hat{h})$ is solution to

$$\int_0^\infty \frac{\left(\frac{T-\tau}{T}\right)\Pr\{\hat{\mathcal{H}}_1\}\log_2 e\gamma}{N_0+\Pr\{\hat{\mathcal{H}}_1\}\sigma_s^2+\bar{P}_1(\hat{g},\hat{h})\gamma} f_{|h|^2|\hat{h}}(\gamma,\hat{h})d\gamma = (\lambda_6+\alpha)\Pr\{\hat{\mathcal{H}}_1\}. \quad (83)$$

Proof: The proposed power allocation scheme can be easily obtained by going through the similar steps as in the proof of Theorem 7. □

IV. Numerical Results

In this section, we present numerical results to illustrate the EE of secondary users attained with the proposed EE maximizing power allocation methods in the presence of imperfect sensing results and different levels of CSI regarding the transmission and interference links. We assume that the prior probabilities of channel being idle and busy, denoted by $\Pr(\mathcal{H}_0)$ and $\Pr(\mathcal{H}_1)$ are 0.6 and 0.4, respectively. This is a reasonable assumption since the Federal Communication Commissions (FCC) report show that the licensed spectrum is underutilized for most of the time [1]. According to spectrum sensing requirements of the cognitive radio-based IEEE 802.22 wireless regional area network, the probability of detection $\mathscr{P}_{\rm d}$ should be at least 90% and false alarm probability $\mathscr{P}_{\rm f}$ should be at most 10% [32]. Therefore, in the simulations, we analyze the impact of detection probability and false alarm probability on the energy efficiency performance of secondary users and consider imperfect sensing decisions with $P_{\rm d}=0.9$ and $P_{\rm f}=0.1$. In addition, according to the IEEE 802.22 standard, we set the sensing duration and frame duration to 1 ms and 10 ms, respectively. The power spectral density of noise is 10^{-8} W/Hz and the channel bandwidth is 6 MHz. The circuit power $P_{\rm c}$ is chosen as 0.1 W [33]. In addition, we consider different range of transmit power and average power constraints in the simulations and the range of SNR values is changed from -11 dBW to 2.76 dBW. It is assumed that the variance of primary user signal is $\sigma_s^2=1$. The step sizes λ and ν are set to 0.1 and tolerance ϵ is chosen as 10^{-6}.

In Fig. 4, we display maximum EE as a function of peak/average transmit power constraints for perfect sensing (i.e., $\mathscr{P}_{\rm d}=1$ and $\mathscr{P}_{\rm f}=0$) and imperfect sensing (i.e., $\mathscr{P}_{\rm d}=0.9$ and $\mathscr{P}_{\rm f}=0.1$). It is assumed that $Q_{\rm avg}=-8$ dBW. Optimal power allocation is performed by assuming perfect instantaneous CSI at the secondary transmitter.

It is seen that perfect detection of the primary user activity results in higher EE compared to the case with imperfect sensing decisions. In particular, the probabilities $\Pr(\mathcal{H}_1|\hat{\mathcal{H}}_0)$ and $\Pr(\mathcal{H}_0|\hat{\mathcal{H}}_1)$ are zero due to perfect spectrum sensing and hence, the secondary users do not experience additive disturbance from primary users, which leads to higher achievable rates, and hence higher EE compared to imperfect sensing case. It is also observed that maximum EE increases with increasing

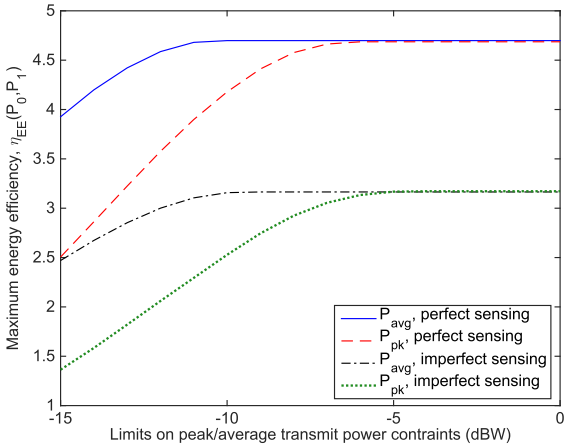

Fig. 4. Maximum EE η_{EE} vs. peak/average transmit power constraints.

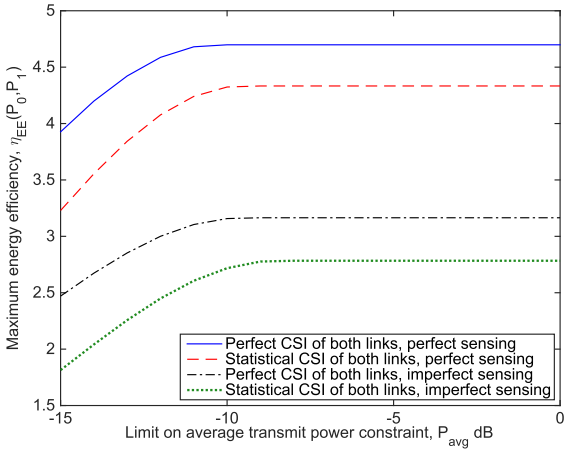

Fig. 5. Maximum EE η_{EE} vs. average transmit power constraint.

peak/average transmit power constraints. When peak/average transmit power constraints become sufficiently large compared to Q_{avg}, maximum EE stays constant since the power is determined by average interference constraint, Q_{avg} rather than peak/average transmit power constraints. Moreover, higher EE is obtained under average transmit power constraint since the optimal power allocation under average transmit power constraint is more flexible than that under peak transmit power constraint.

In Fig. 5, we plot maximum EE attained with the proposed optimal power allocation schemes as a function of the average transmit power constraint under perfect sensing with $\mathscr{P}_{\text{d}} = 1$ and $\mathscr{P}_{\text{f}} = 0$) and imperfect sensing with $\mathscr{P}_{\text{d}} = 0.9$ and $\mathscr{P}_{\text{f}} = 0.1$. We assume the availability of either perfect instantaneous CSI or statistical CSI of both transmission and interference links at the secondary transmitter. Q_{avg} is set to -25 dBW. It is observed from the figure that when the optimal power allocation with perfect instantaneous CSI is applied, higher EE is achieved compared to the optimal power allocation with statistical CSI. More specifically, the power allocation scheme assuming perfect instantaneous CSI can exploit favorable channel conditions and higher transmission power is allocated to better channel, and hence a secondary user's power budget is more efficiently utilized compared to the power allocation scheme assuming statistical CSI in which the power levels do not change according to channel conditions. It is also seen that imperfect sensing decisions significantly affect the performance of secondary users, resulting in lower EE under both optimal power allocation strategies.

In Fig. 6, we display maximum EE, achievable rate R_a, and optimal powers, P_{tot}, P_0 and P_1 as a function of detection probability, $\mathscr{P}_{\text{d}}$. It is assumed that peak transmit power constraints are $P_{\text{pk},0} = P_{\text{pk},1} = -4$ dBW and average interference power constraint is $Q_{\text{avg}} = -25$ dBW. In addition, probability of false alarm, $\mathscr{P}_{\text{f}}$ is set to 0.1. We consider the power allocation schemes for the following four cases: (1) perfect CSI of both transmission and interference links; (2) perfect CSI of the transmission link and imperfect CSI of the interference link; (3) imperfect CSI of both transmission and interference links; and (4) only statistical CSI of both transmission and interference links. We only plot optimal powers, P_{tot}, P_0 and P_1 for the optimal power allocation with perfect instantaneous CSI of both links since the same trend is observed under the assumption of other CSI levels. As $\mathscr{P}_{\text{d}}$ increases, secondary users have more reliable sensing performance. Hence, secondary users experience miss detection events less frequently, which results in increased achievable rate. The transmission power under idle sensing decision, P_0 increases with increasing $\mathscr{P}_{\text{d}}$ while transmission power under busy sensing decision, P_1 decreases with increasing $\mathscr{P}_{\text{d}}$. Since achievable rate increases and total transmission power slightly increases, maximum EE of secondary users increases as sensing performance improves. It is also seen that the power allocation scheme with perfect instantaneous CSI of both links outperforms the other proposed power allocation strategies. Moreover, the performance of secondary users in terms of throughput and EE degrades gradually as we have less and less information regarding the transmission and interference links at the secondary transmitter.

Fig. 7 shows maximum EE, achievable rate, R_a and optimal powers, P_{tot}, P_0 and P_1 as a function of false alarm probability, $\mathscr{P}_{\text{f}}$. We consider the same setting as in the previous figure. It is again assumed that $P_{pk,0} = P_{\text{pk},1} = -4$ dBW and $Q_{\text{avg}} = -8$ dBW. Since optimal powers maximizing EE show similar trends as a function of $\mathscr{P}_{\text{f}}$, we only plot the optimal power levels under the assumption of perfect instantaneous CSI of both transmission and interference links in Fig. 7 (c). Probability of detection, $\mathscr{P}_{\text{d}}$ is chosen as 0.9. As $\mathscr{P}_{\text{f}}$ increases, channel sensing performance deteriorates. In this case, secondary users detect the channel as busy more frequently even if the channel is idle. Total transmission power maximizing EE slightly decreases with increasing $\mathscr{P}_{\text{f}}$. In addition, since the available channel is not utilized efficiently, secondary users have smaller achievable rate, which leads to lower achievable EE. Again, the power allocation scheme with perfect instantaneous CSI of both links gives the best performance in terms of throughput and EE.

In Fig. 8, we display maximum EE as a function of channel estimation error variance of the interference link. Power allocation is employed by perfect CSI of transmission link and imperfect CSI of interference link, and imperfect

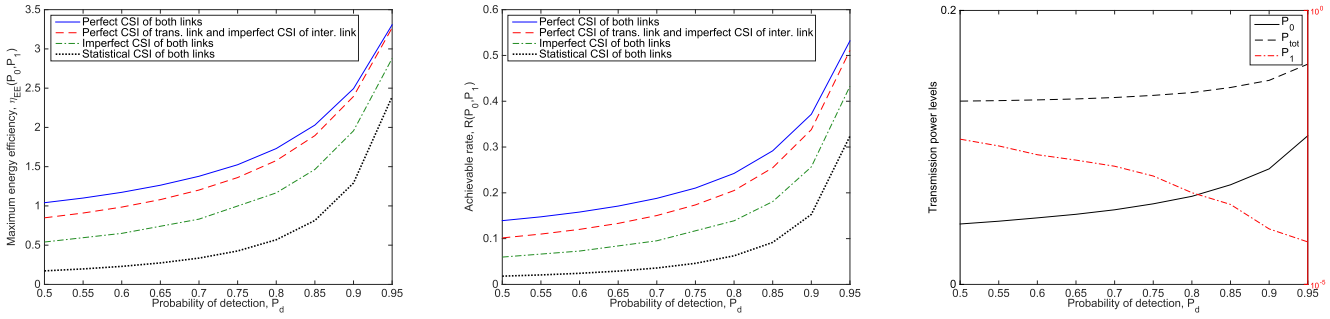

(a) (b) (c)

Fig. 6. (a) Maximum achievable EE, η_{EE} vs. probability of detection, $\mathscr{P}_{\text{d}}$; (b) achievable rate maximizing EE, R_a vs. $\mathscr{P}_{\text{d}}$; (c) optimal total transmission power, P_{tot} and P_0, P_1 vs. $\mathscr{P}_{\text{d}}$.

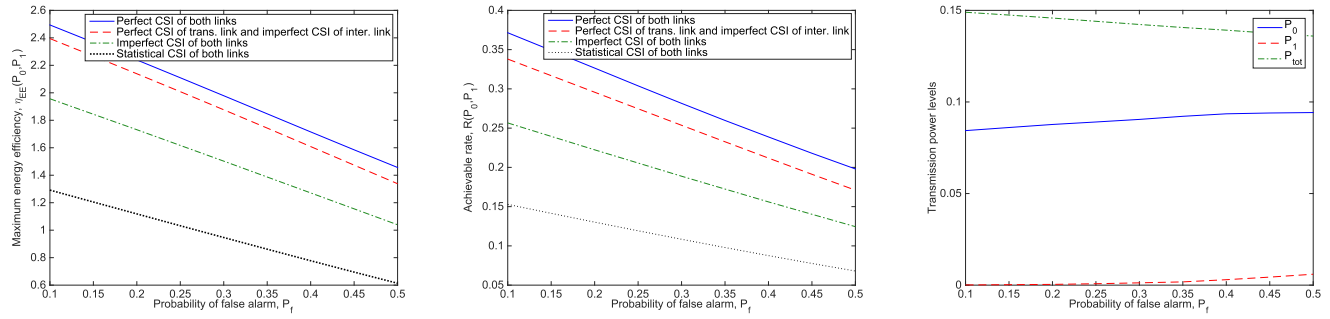

(a) (b) (c)

Fig. 7. (a) Maximum EE, η_{EE} vs. probability of false alarm, $\mathscr{P}_{\text{f}}$; (b) achievable rate maximizing EE, R_a vs. $\mathscr{P}_{\text{f}}$; (c) optimal total transmission power, P_{tot} and P_0, P_1 vs. $\mathscr{P}_{\text{f}}$.

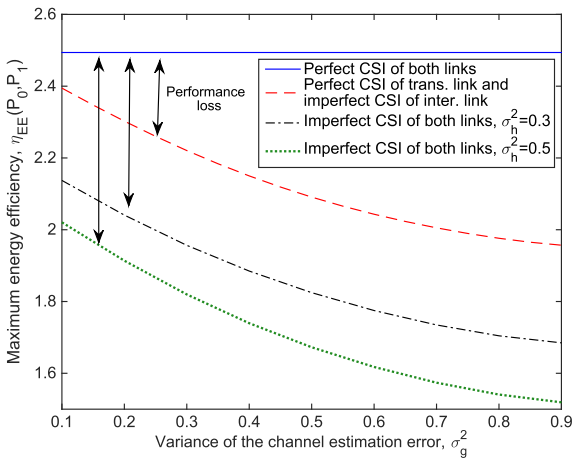

Fig. 8. Maximum EE η_{EE} vs. channel estimation error variance of the interference link, σ_g^2.

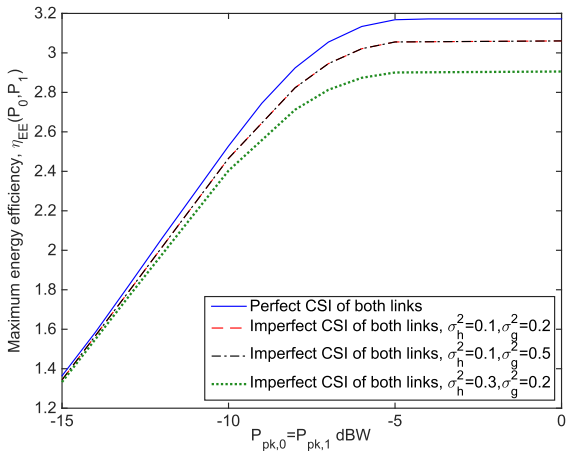

Fig. 9. Maximum EE η_{EE} vs. peak transmit power constraints, $P_{\text{pk},0} = P_{\text{pk},1}$.

CSI of both links with $\sigma_h^2 = 0.3$ and $\sigma_h^2 = 0.5$. We assume that $P_{pk,0} = P_{\text{pk},1} = -4$ dBW and $Q_{\text{avg}} = -25$ dBW, and sensing is imperfect with $\mathscr{P}_{\text{d}} = 0.9$ and $\mathscr{P}_{\text{f}} = 0.1$. The EE attained with the optimal power allocation assuming perfect CSI of both links is displayed as a baseline to compare the performance loss due to imperfect CSI of either interference link or of both transmission and interference links at the secondary transmitter. It is observed that EE of secondary users decreases as the variance of the channel estimation error in the interference link, σ_g^2, increases and hence the channel estimate becomes less accurate. The secondary users even have lower EE when CSI of both links are imperfectly known. Therefore, accurate estimation of both transmission and interference links is crucial in order to achieve better EE.

Fig. 9 shows the maximum EE as a function of the peak transmit power constraints, $P_{\text{pk},0} = P_{\text{pk},1}$ under imperfect

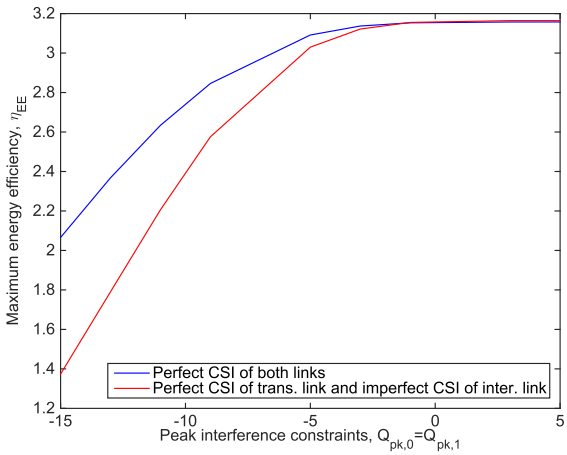

Fig. 10. Maximum EE η_{EE} vs. peak interference power constraints, $Q_{\text{pk},0} = Q_{\text{pk},1}$.

sensing result (i.e., when $\mathscr{P}_{\text{d}} = 0.9$ and $\mathscr{P}_{\text{f}} = 0.1$). We consider the optimal power allocation schemes assuming either perfect CSI of both links or imperfect CSI of both links with $\sigma_h^2 = 0.1$ and $\sigma_g^2 = 0.2$, $\sigma_h^2 = 0.1$ and $\sigma_g^2 = 0.5$, and $\sigma_h^2 = 0.3$ and $\sigma_g^2 = 0.2$. Average interference constraint, Q_{avg} is set to -10 dBW. When channel estimation error of the transmission link increases from 0.1 and 0.3 keeping $\sigma_g^2 = 0.2$, EE of secondary users decreases more compared to the case when the channel estimation error of the interference link increases from 0.2 to 0.5 while $\sigma_h^2 = 0.1$ since the average interference constraint is loose, and imperfect CSI of the interference link only slightly affects the performance. Also, as P_{pk} increases, EE of secondary users first increases and then stays constant since average transmission power reaches to the value that maximizes EE. Therefore, further increasing P_{pk} does not provide any EE improvement.

In Fig. 10, we plot the maximum EE as a function of the peak interference power constraints, $Q_{\text{pk},0} = Q_{\text{pk},1}$. It is assumed that $\mathscr{P}_{\text{d}} = 0.9$ and $\mathscr{P}_{\text{f}} = 0.1$. We consider that either perfect instantaneous CSI of both links or perfect CSI of transmission link and imperfect CSI of interference link is available at the secondary transmitter. We set $P_{\text{avg}} = -10$ dBW, outage thresholds $\xi_0 = \xi_1 = 0.1$ and $\sigma_g^2 = 0.1$. It is seen that EE curves under both cases first increase with increasing interference power constraints, and then level and approach the same value due to average transmit power constraint. Also, the availability of only imperfect CSI of the interference link deteriorates the system performance and leads to lower EE compared to that with perfect CSI of the interference link.

V. Conclusion

In this paper, we determine energy-efficient power allocation schemes for cognitive radio systems subject to peak/average transmit power and peak/average interference power constraints in the presence of sensing errors and different levels of CSI regarding the transmission and interference links. A low-complexity algorithm based on Dinkelbach's method is proposed to iteratively solve the power allocation that maximizes EE.

We have obtained several important insights through the proposed power control schemes. In particular, the power allocation levels in the case of perfect CSI have the structure of the water-filling policy with water level being determined by the channel power gain of the interference link. However, in contrast to throughput maximization, average power constraint is not necessarily satisfied with equality in the case of EE maximization. Also, the power allocation scheme obtained under instantaneous CSI of both links leads to higher EE compared to that with statistical CSI since favorable channel conditions can be exploited and transmission powers can be adapted according to the channel variations. The proposed power levels depend on channel estimation errors under imperfect CSI of both transmission and interference links. Setting the estimation errors to zero, the power control scheme under perfect CSI of both links is recovered. In addition, outage threshold affects the power allocation schemes subject to peak interference power constraint under imperfect CSI of the interference link. More specifically, the secondary users transmit with higher power as the outage threshold increases. It is also shown that power allocation schemes depend on sensing performance through detection and false alarm probabilities.

Numerical results reveal interesting relations and trade-offs. For instance, it is shown that maximum achievable EE increases with increasing $\mathscr{P}_{\text{d}}$ and decreases with increasing $\mathscr{P}_{\text{f}}$. Imperfect CSI of the transmission and interference links significantly degrades the performance of secondary users in terms of EE. Therefore, accurate estimation of the transmission and interference links is of great importance in order to obtain higher EE. Moreover, under the same average interference constraint, secondary users' transmission subject to peak transmit constraint achieves smaller achievable EE than that under average transmit power constraint.

Appendix

A. Proof of Proposition 1

We first write the achievable rate of secondary users in terms of mutual information between the received and transmitted signals given the sensing decision as follows:

$$R_G = \frac{T-\tau}{T} I(x; y|h, \hat{\mathcal{H}}) = \frac{T-\tau}{T}\Big[\Pr\{\hat{\mathcal{H}}_0\} I(x_0; y|h, \hat{\mathcal{H}}_0) + \Pr\{\hat{\mathcal{H}}_1\} I(x_1; y|h, \hat{\mathcal{H}}_1)\Big], \quad (84)$$

where $I(x_k; y|h, \hat{\mathcal{H}}_k)$ for $k \in \{0, 1\}$ can be further expressed as

$$I(x_k; y|h, \hat{\mathcal{H}}_k) = \mathbb{E}_{x_k, y, g, h}\left\{ \log_2 \left(\frac{f(y|x_k, h, \hat{\mathcal{H}}_k)}{f(y|h, \hat{\mathcal{H}}_k)} \right) \right\}. \quad (85)$$

The above conditional distribution, $f(y|x_k, h, \hat{\mathcal{H}}_k)$, is determined through the input-output relation in (5) as follows:

$$f(y|x_k, h, \hat{\mathcal{H}}_k) = \frac{\Pr\{\mathcal{H}_0|\hat{\mathcal{H}}_k\}}{\pi N_0} \mathrm{e}^{-\frac{|y-hx_k|^2}{N_0}} + \frac{\Pr\{\mathcal{H}_1|\hat{\mathcal{H}}_k\}}{\pi (N_0+\sigma_s^2)} \mathrm{e}^{-\frac{|y-hx_k|^2}{N_0+\sigma_s^2}} \quad (86)$$

with variance

$$\mathbb{E}\{|y|^2|x_k,h,\hat{\mathcal{H}}_k\}=N_0+\Pr\{\mathcal{H}_1|\hat{\mathcal{H}}_k\}\sigma_s^2. \quad (87)$$

Also, assuming Gaussian distributed input, the conditional distribution, $f(y|h,\hat{\mathcal{H}}_k)$ in (85) is given by

$$f(y|h,\hat{\mathcal{H}}_k)=\frac{\Pr\{\mathcal{H}_0|\hat{\mathcal{H}}_k\}}{\pi(N_0+P_k(g,h)|h|^2)}\mathrm{e}^{-\frac{|y|^2}{N_0+P_k(g,h)|h|^2}}+\frac{\Pr\{\mathcal{H}_1|\hat{\mathcal{H}}_k\}}{\pi(N_0+P_k(g,h)|h|^2+\sigma_s^2)}\mathrm{e}^{-\frac{|y|^2}{N_0+P_k(g,h)|h|^2+\sigma_s^2}} \quad (88)$$

with variance

$$\mathbb{E}\{|y|^2|h,\hat{\mathcal{H}}_k\}=N_0+P_k(g,h)|h|^2+\Pr\{\mathcal{H}_1|\hat{\mathcal{H}}_k\}\sigma_s^2. \quad (89)$$

Above, it is seen that the conditional distributions of the received signal y given sensing decisions become a mixture of Gaussian distributions due to channel sensing errors. Therefore, there is no closed form expression for mutual information in (85). However, we can still find a closed-form lower bound for the achievable rate expression by following the steps in [22, pp. 938–939] and replacing the additive disturbance w in (6) with the worst-case Gaussian noise with the same variance as follows:

$$I(x_k;y|h,\hat{\mathcal{H}}_k)\geq\mathbb{E}_{g,h}\left\{\log_2\left(1+\frac{P_k(g,h)|h|^2}{E\{|w|^2|\hat{\mathcal{H}}_k\}}\right)\right\} \quad (90)$$

where

$$E\{|w|^2|\hat{\mathcal{H}}_k\}=N_0+\Pr\{\mathcal{H}_1|\hat{\mathcal{H}}_k\}\sigma_s^2. \quad (91)$$

Inserting these lower bounds into (84), we have obtained the achievable rate expression in (8). □

B. Proof of Theorem 1

We first express $I_0(x_0;y|h,\hat{\mathcal{H}}_0)$ as in (84), where $c_1=N_0+\sigma_s^2$ and $c_2=N_0$. Then, using (92), shown at the bottom of the page, and the following inequalities:

$$\mathrm{e}^{-\frac{|y|^2}{c_1+|h|^2P_0(g,h)}}\geq\mathrm{e}^{-\frac{|y|^2}{c_i+|h|^2P_0(g,h)}}\geq\mathrm{e}^{-\frac{|y|^2}{c_2+|h|^2P_0(g,h)}} \quad (93)$$

$$\mathrm{e}^{-\frac{|y-hx_0|^2}{c_1}}\geq\mathrm{e}^{-\frac{|y-hx_0|^2}{c_i}}\geq\mathrm{e}^{-\frac{|y-hx_0|^2}{c_2}}, \quad (94)$$

we obtain the upper bound in (95) shown at the top of next page.

Evaluating the integrals in (95) yields the upper bound in (96), shown at the bottom of this page. Following the similar steps, we obtain the upper bound for $I_1(x_1;y|h,\hat{\mathcal{H}}_1)$ in (97), shown at the top of the next page. Inserting the inequalities in (95) and (97) into (84) and subtracting R_a in (8) give the desired result in (11). □

C. Proof of Theorem 2

The optimization problem is quasiconcave since achievable rate R_a is concave in transmission powers and total power consumption $P_{\mathrm{tot}}(P_0,P_1)$ is both affine and positive, and hence the level sets $S_\alpha=\{(P_0,P_1):\eta_{\mathrm{EE}}\geq\alpha\}=\{\alpha P_{\mathrm{tot}}(P_0,P_1)-R_a\leq 0\}$ are convex for any $\alpha\in\mathbb{R}$. Since quasiconcave functions have more than one local maximum, local maximum does not always guarantee the global maximum. Therefore, standard convex optimization algorithms cannot be directly used. Hence, iterative power allocation algorithm based on Dinkelbach's method [23] is employed to solve the quasiconcave EE maximization problem by formulating the equivalent parameterized concave problem as follows:

$$\max_{\substack{P_0(g,h)\\P_1(g,h)}}\Big\{\mathbb{E}_{g,h}\big\{R\big(P_0(g,h),P_1(g,h)\big)\big\}-\alpha(\mathbb{E}_{g,h}\{\Pr\{\hat{\mathcal{H}}_0\}P_0(g,h)+\Pr\{\hat{\mathcal{H}}_1\}P_1(g,h)\}+P_{\mathrm{c}})\Big\} \quad (98)$$

subject to

$$\mathbb{E}_{g,h}\{\Pr\{\hat{\mathcal{H}}_0\}\,P_0(g,h)+\Pr\{\hat{\mathcal{H}}_1\}\,P_1(g,h)\}\leq P_{\mathrm{avg}} \quad (99)$$

$$\mathbb{E}_{g,h}\{\big[(1-\mathscr{P}_{\mathrm{d}})\,P_0(g,h)+\mathscr{P}_{\mathrm{d}}\,P_1(g,h)\big]|g|^2\}\leq Q_{\mathrm{avg}} \quad (100)$$

$$P_0(g,h)\geq 0,\quad P_1(g,h)\geq 0, \quad (101)$$

$$I_0(x_0;y|h,\hat{\mathcal{H}}_0)=\Big(\frac{T-\tau}{T}\Big)\Big[\int_h\Big(\int_{-\infty}^{\infty}\sum_{i=1}^{2}\frac{\Pr(\mathcal{H}_i|\hat{\mathcal{H}}_0)}{\pi c_i}\mathrm{e}^{-\frac{|y-x_0h|^2}{c_i}}\log_2\Big(\sum_{i=1}^{2}\frac{\Pr(\mathcal{H}_i|\hat{\mathcal{H}}_0)}{\pi c_i}\mathrm{e}^{-\frac{|y-x_0h|^2}{c_i}}\Big)dy\Big)f_h(h)dh-\int_g\Big(\int_h\Big(\int_{-\infty}^{\infty}\sum_{i=1}^{2}\frac{\Pr(\mathcal{H}_i|\hat{\mathcal{H}}_0)}{\pi(c_i+|h|^2P_0(g,h))}\mathrm{e}^{-\frac{|y|^2}{c_i+|h|^2P_0(g,h)}}\log_2\Big(\sum_{i=1}^{2}\frac{\Pr(\mathcal{H}_i|\hat{\mathcal{H}}_0)}{\pi(c_i+|h|^2P_0(g,h))}\mathrm{e}^{-\frac{|y|^2}{c_i+|h|^2P_0(g,h)}}\Big)dy\Big)f_h(h)dh\Big)f_g(g)dg\Big], \quad (92)$$

$$I_0(x_0;y|h,\hat{\mathcal{H}}_0)\leq\Big(\frac{T-\tau}{T}\Big)\Big[\int_h\Big(\int_{-\infty}^{\infty}\sum_{i=1}^{2}\frac{\Pr(\mathcal{H}_i|\hat{\mathcal{H}}_0)}{\pi c_i}\mathrm{e}^{-\frac{|y-x_0h|^2}{c_i}}\log_2\Big(\sum_{i=1}^{2}\frac{\Pr(\mathcal{H}_i|\hat{\mathcal{H}}_0)}{\pi c_i}\mathrm{e}^{-\frac{|y-x_0h|^2}{c_1}}\Big)dy\Big)f_h(h)dh-\int_g\Big(\int_h\Big(\int_{-\infty}^{\infty}\sum_{i=1}^{2}\frac{\Pr(\mathcal{H}_i|\hat{\mathcal{H}}_0)}{\pi(c_i+|h|^2P_0(g,h))}\mathrm{e}^{-\frac{|y|^2}{c_i+|h|^2P_0(g,h)}}\log_2\Big(\sum_{i=1}^{2}\frac{\Pr(\mathcal{H}_i|\hat{\mathcal{H}}_0)}{\pi(c_i+|h|^2P_0(g,h))}\mathrm{e}^{-\frac{|y|^2}{c_2+|h|^2P_0(g,h)}}\Big)dy\Big)f_h(h)dh\Big)f_g(g)dg\Big]. \quad (95)$$

$$I_0(x_0;\, y|h, \hat{\mathcal{H}}_0) \leq \left(\frac{T-\tau}{T}\right)\left[\mathbb{E}_{g,h}\left\{\sum_{k=1}^{2}\log_2\left(\frac{\sum_{i=1}^{2}\frac{\Pr(\mathcal{H}_i|\hat{\mathcal{H}}_0)}{c_i}}{\sum_{i=1}^{2}\frac{\Pr(\mathcal{H}_i|\hat{\mathcal{H}}_0)}{c_i+|h|^2P_0(g,h)}}\right)\right\} - \left(\frac{N_0+\Pr(H_1|\hat{\mathcal{H}}_0)\sigma_s^2}{N_0+\sigma_s^2}\right) + \mathbb{E}_{g,h}\left\{1+\frac{\Pr(H_1|\hat{\mathcal{H}}_0)\sigma_s^2}{N_0+|h|^2P_0(g,h)}\right\}\right] \quad (96)$$

$$I_1(x_1;\, y|h, \hat{\mathcal{H}}_1) \leq \left(\frac{T-\tau}{T}\right)\left[\mathbb{E}_{g,h}\left\{\sum_{k=1}^{2}\log_2\left(\frac{\sum_{i=1}^{2}\frac{\Pr(\mathcal{H}_i|\hat{\mathcal{H}}_1)}{c_i}}{\sum_{i=1}^{2}\frac{\Pr(\mathcal{H}_i|\hat{\mathcal{H}}_1)}{c_i+|h|^2P_1(g,h)}}\right)\right\} - \left(\frac{N_0+\Pr(H_1|\hat{\mathcal{H}}_1)\sigma_s^2}{N_0+\sigma_s^2}\right) + \mathbb{E}_{g,h}\left\{1+\frac{\Pr(H_1|\hat{\mathcal{H}}_1)\sigma_s^2}{N_0+|h|^2P_1(g,h)}\right\}\right] \quad (97)$$

where α is a nonnegative parameter. At the optimal value of α^*, solving the EE maximization problem in (13) is equivalent to solving the above parametrized concave problem if and only if the following condition is satisfied

$$F(\alpha^*) = \mathbb{E}_{g,h}\left\{R\big(P_0(g,h),\, P_1(g,h)\big)\right\} - \alpha^*\Big(\mathbb{E}_{g,h}\{\Pr\{\hat{\mathcal{H}}_0\}P_0(g,h) + \Pr\{\hat{\mathcal{H}}_1\}P_1(g,h)\} + P_{\mathrm{c}}\Big) = 0. \quad (102)$$

The detailed proof of the above condition is available in [23]. Since the problem in (98) is concave, the optimal power values are obtained by forming the Lagrangian as follows:

$$\begin{aligned} &L(P_0,\, P_1,\, \lambda_1,\, \nu_1,\, \alpha) \\ &= \mathbb{E}_{g,h}\left\{R\big(P_0(g,h),\, P_1(g,h)\big)\right\} \\ &\quad - \alpha(\mathbb{E}_{g,h}\{\Pr\{\hat{\mathcal{H}}_0\}P_0(g,h) + \Pr\{\hat{\mathcal{H}}_1\}P_1(g,h)\} + P_{\mathrm{c}}) \\ &\quad - \lambda_1(\mathbb{E}_{g,h}\{\Pr\{\hat{\mathcal{H}}_0\}\,P_0(g,h) + \Pr\{\hat{\mathcal{H}}_1\}\,P_1(g,h)\} - P_{\mathrm{avg}}) \\ &\quad - \nu_1(\mathbb{E}_{g,h}\{\left[(1-\mathscr{P}_{\mathrm{d}})\,P_0(g,h) + \mathscr{P}_{\mathrm{d}}\,P_1(g,h)\right]|g|^2\} - Q_{\mathrm{avg}}), \end{aligned} \quad (103)$$

where λ_1 and ν_1 are nonnegative Lagrange multipliers. According to the Karush-Kuhn-Tucker (KKT) conditions, the optimal values of $P_0^*(g,h)$ and $P_1^*(g,h)$ satisfy the following equations:

$$\frac{\frac{T-\tau}{T}\Pr\{\hat{\mathcal{H}}_0\}|h|^2\log_2 e}{N_0+\Pr(\mathcal{H}_1|\hat{\mathcal{H}}_0)\sigma_s^2+P_0^*(g,h)|h|^2} - (\lambda_1+\alpha)\Pr\{\hat{\mathcal{H}}_0\} - \nu_1|g|^2(1-\mathscr{P}_{\mathrm{d}}) = 0 \quad (104)$$

$$\frac{\frac{T-\tau}{T}\Pr\{\hat{\mathcal{H}}_1\}|h|^2\log_2 e}{N_0+\Pr(\mathcal{H}_1|\hat{\mathcal{H}}_1)\sigma_s^2+P_1^*(g,h)|h|^2} - (\lambda_1+\alpha)\Pr\{\hat{\mathcal{H}}_1\} - \nu_1|g|^2\mathscr{P}_{\mathrm{d}} = 0 \quad (105)$$

$$\lambda_1(\mathbb{E}\{\Pr\{\hat{\mathcal{H}}_0\}\,P_0^*(g,h) + \Pr\{\hat{\mathcal{H}}_1\}\,P_1^*(g,h)\} - P_{\mathrm{avg}}) = 0 \quad (106)$$

$$\nu_1(\mathbb{E}\{[(1-\mathscr{P}_{\mathrm{d}})\,P_0^*(g,h) + \mathscr{P}_{\mathrm{d}}\,P_1^*(g,h)]|g|^2\} - Q_{\mathrm{avg}}) = 0 \quad (107)$$

$$\lambda_1 \geq 0, \quad \nu_1 \geq 0. \quad (108)$$

Solving equations (104) and (105), yield the optimal power values in (17) and (18), respectively. □

REFERENCES

[1] *Report of the Spectrum Efficiency Working Group*, Federal Commun. Commission Spectrum Policy Task Force, Washington, DC, USA, Nov. 2002.

[2] J. Mitola, III, "Cognitive radio: An integrated agent architecture for software defined radio," Ph.D. dissertation, Dept. Teleinformat. Comput. Commun. Syst. Lab., Roy. Inst. Technol., Stockholm, Sweden, 2000.

[3] S. Haykin, "Cognitive radio: Brain-empowered wireless communications," *IEEE J. Sel. Areas Commun.*, vol. 23, no. 2, pp. 201–220, Feb. 2005.

[4] G. Gür and F. Alagöz, "Green wireless communications via cognitive dimension: An overview," *IEEE Netw.*, vol. 25, no. 2, pp. 50–56, Mar./Apr. 2011.

[5] X. Hong, J. Wang, C.-X. Wang, and J. Shi, "Cognitive radio in 5G: A perspective on energy-spectral efficiency trade-off," *IEEE Commun. Mag.*, vol. 52, no. 7, pp. 46–53, Jul. 2014.

[6] Y. Pei, Y.-C. Liang, K. C. Teh, and K. H. Li, "Energy-efficient design of sequential channel sensing in cognitive radio networks: Optimal sensing strategy, power allocation, and sensing order," *IEEE J. Sel. Areas Commun.*, vol. 29, no. 8, pp. 1648–1659, Sep. 2011.

[7] Z. Shi, K. C. Teh, and K. H. Li, "Energy-efficient joint design of sensing and transmission durations for protection of primary user in cognitive radio systems," *IEEE Commun. Lett.*, vol. 17, no. 3, pp. 565–568, Mar. 2013.

[8] S. Wang, M. Ge, and W. Zhao, "Energy-efficient resource allocation for OFDM-based cognitive radio networks," *IEEE Trans. Commun.*, vol. 61, no. 8, pp. 3181–3191, Aug. 2013.

[9] F. Gabry, A. Zappone, R. Thobaben, E. A. Jorswieck, and M. Skoglund, "Energy efficiency analysis of cooperative jamming in cognitive radio networks with secrecy constraints," *IEEE Wireless Commun. Lett.*, vol. 4, no. 4, pp. 437–440, Aug. 2015.

[10] C. Xiong, L. Lu, and G. YE. Li, "Energy-efficient spectrum access in cognitive radios," *IEEE J. Sel. Areas Commun.*, vol. 32, no. 3, pp. 550–562, Mar. 2014.

[11] R. Ramamonjison and V. K. Bhargava, "Energy efficiency maximization framework in cognitive downlink two-tier networks," *IEEE Trans. Wireless Commun.*, vol. 14, no. 3, pp. 1468–1479, Mar. 2015.

[12] J. Mao, G. Xie, J. Gao, and Y. Liu, "Energy efficiency optimization for cognitive radio MIMO broadcast channels," *IEEE Commun. Lett.*, vol. 17, no. 2, pp. 337–340, Feb. 2013.

[13] X. Kang, Y. C. Liang, H. K. Garg, and L. Zhang, "Sensing-based spectrum sharing in cognitive radio networks," *IEEE Trans. Veh. Technol.*, vol. 58, no. 8, pp. 4649–4654, Oct. 2009.

[14] S. Stotas and A. Nallanathan, "Optimal sensing time and power allocation in multiband cognitive radio networks," *IEEE Trans. Commun.*, vol. 59, no. 1, pp. 226–235, Jan. 2011.

[15] H. Chen, L. Liu, J. Matyjas, and M. Medley, "Optimal resource allocation for sensing based spectrum sharing cognitive radio networks," in *Proc. IEEE Global Commun. Conf. (Globecom)*, Dec. 2014, pp. 899–904.

[16] E. Bedeer, O. Amin, O. A. Dobre, M. H. Ahmed, and K. E. Baddour, "Energy-efficient power loading for OFDM-based cognitive radio systems with channel uncertainties," *IEEE Trans. Veh. Technol.*, vol. 64, no. 6, pp. 2672–2677, Jun. 2015.

[17] R. Ramamonjison and V. K. Bhargava, "Sum energy-efficiency maximization for cognitive uplink networks with imperfect CSI," in *Proc. IEEE Wireless Commun. Netw. Conf. (WCNC)*, Apr. 2014, pp. 1012–1017.

[18] M. R. Mili, L. Musavian, K. A. Hamdi, and F. Marvasti, "How to increase energy efficiency in cognitive radio networks," *IEEE Trans. Commun.*, vol. 64, no. 5, pp. 1829–1843, May 2016.
[19] L. Wang, M. Sheng, Y. Zhang, X. Wang, and C. Xu, "Robust energy efficiency maximization in cognitive radio networks: The worst-case optimization approach," *IEEE Trans. Commun.*, vol. 63, no. 1, pp. 51–65, Jan. 2015.
[20] A. Ghasemi and E. S. Sousa, "Spectrum sensing in cognitive radio networks: Requirements, challenges and design trade-offs," *IEEE Commun. Mag.*, vol. 46, no. 4, pp. 32–39, Apr. 2008.
[21] E. Axell, G. Leus, E. G. Larsson, and H. V. Poor, "Spectrum sensing for cognitive radio: State-of-the-art and recent advances," *IEEE Signal Process. Mag.*, vol. 29, no. 3, pp. 101–116, May 2012.
[22] M. Medard, "The effect upon channel capacity in wireless communications of perfect and imperfect knowledge of the channel," *IEEE Trans. Inf. Theory*, vol. 46, no. 3, pp. 933–946, May 2000.
[23] W. Dinkelbach, "On nonlinear fractional programming," *Manage. Sci.*, vol. 13, no. 7, pp. 492–498, Mar. 1967.
[24] S. Boyd, L. Xiao, and A. Mutapcic, "Subgradient methods," Stanford Univ., Stanford, CA, USA, Tech. Rep. EE392o, 2004.
[25] S. Schaible, "Fractional programming. II, On Dinkelbach's algorithm," *Manage. Sci.*, vol. 22, no. 8, pp. 868–873, 1976.
[26] X. Zhao, P. B. Luh, and J. Wang, "Surrogate gradient algorithm for Lagrangian relaxation," *J. Optim. Theory Appl.*, vol. 100, no. 3, pp. 699–712, Mar. 1999.
[27] X. Kang, Y. C. Liang, A. Nallanathan, H. K. Garg, and R. Zhang, "Optimal power allocation for fading channels in cognitive radio networks: Ergodic capacity and outage capacity," *IEEE Trans. Wireless Commun.*, vol. 8, no. 2, pp. 940–950, Feb. 2009.
[28] L. Musavian and S. Aissa, "Fundamental capacity limits of cognitive radio in fading environments with imperfect channel information," *IEEE Trans. Commun.*, vol. 57, no. 11, pp. 3472–3480, Nov. 2009.
[29] H. A. Suraweera, P. J. Smith, and M. Shafi, "Capacity limits and performance analysis of cognitive radio with imperfect channel knowledge," *IEEE Trans. Veh. Technol.*, vol. 59, no. 4, pp. 1811–1822, May 2010.
[30] M. Abramowitz and I. A. Stegun, Eds., *Handbook of Mathematical Functions: With Formulas, Graphs, and Mathematical Tables*. New York, NY, USA: Dover, 1972.
[31] L. Sboui, Z. Rezki, and M. S. Alouini, "A unified framework for the ergodic capacity of spectrum sharing cognitive radio systems," *IEEE Trans. Wireless Commun.*, vol. 12, no. 2, pp. 877–887, Feb. 2013.
[32] *Standard for Wireless Regional Area Networks (WRAN)—Specific Requirements—Part 22: Cognitive Wireless RAN Medium Access Control (MAC) and Physical Layer (PHY) Specifications: Policies and Procedures for Operation in the TV Bands*, IEEE Standard 802.22, The Institute of Electrical and Electronics Engineering, Inc., 2005.
[33] X. Lu, P. Wang, D. Niyato, D. I. Kim, and Z. Han, "Wireless networks with RF energy harvesting: A contemporary survey," *IEEE Commun. Surveys Tut.*, vol. 17, no. 2, pp. 757–789, 2nd Quart., 2014.

Gozde Ozcan received the B.S. degree from Bilkent University, Turkey, in 2011, and the Ph.D. degree in electrical engineering from Syracuse University in 2016. She was a Research Intern with Mitsubishi Electric Research Laboratories, Cambridge, MA, USA, from 2015 to 2016. Her research interests include wireless communications, radio resource management, energy-efficient transmission techniques, statistical signal processing, machine learning, and cognitive radio systems. She has been a TPC member of VTC'2014-Fall and VTC'2017-Spring.

M. Cenk Gursoy received the B.S. degree (Hons.) in electrical and electronics engineering from Bogazici University, Istanbul, Turkey, in 1999, and the Ph.D. degree in electrical engineering from Princeton University, Princeton, NJ, USA, in 2004. In 2000, he was with Lucent Technologies, Holmdel, NJ, where he conducted performance analysis of DSL modems. From 2004 to 2011, he was a Faculty Member with the Department of Electrical Engineering, University of Nebraska–Lincoln. He is currently an Associate Professor with the Department of Electrical Engineering and Computer Science, Syracuse University. His research interests are in the general areas of wireless communications, information theory, communication networks, and signal processing. He is currently a member of the editorial boards of the IEEE TRANSACTIONS ON GREEN COMMUNICATIONS AND NETWORKING, the IEEE TRANSACTIONS ON COMMUNICATIONS, the IEEE TRANSACTIONS ON VEHICULAR TECHNOLOGY, the IEEE JOURNAL ON SELECTED AREAS IN COMMUNICATIONS–SERIES ON GREEN COMMUNICATIONS AND NETWORKING, and the *Physical Communication* (Elsevier). He served as an Editor of the IEEE TRANSACTIONS ON WIRELESS COMMUNICATIONS from 2010 to 2015 and the IEEE COMMUNICATIONS LETTERS from 2012 to 2014. He received the NSF CAREER Award in 2006, the *EURASIP Journal of Wireless Communications and Networking* Best Paper Award, the UNL College Distinguished Teaching Award, and the Maude Hammond Fling Faculty Research Fellowship. He was a recipient of the Gordon Wu Graduate Fellowship from Princeton University from 1999 to 2003.

Nghi Tran received the B.Eng. degree from the Hanoi University of Technology, Hanoi, Vietnam, in 2002, and the M.Sc. and Ph.D. degrees from the University of Saskatchewan, Saskatoon, SB, Canada, in 2004 and 2008, respectively, all in electrical and computer engineering. From 2008 to 2010, he was a Post-Doctoral Scholar under the prestigious Natural Sciences and Engineering Research Council of Canada Post-Doctoral Fellowship with McGill University, where he was a Research Associate from 2010 to 2011. He was a Consultant with the satellite industry. Since 2011, he has been an Assistant Professor with the Department of Electrical and Computer Engineering, The University of Akron, Akron, OH, USA. His research interests span the areas of signal processing and communication and information theories for wireless systems and networks. He was a recipient of the Graduate Thesis Award from the University of Saskatchewan. He is currently an Editor of the IEEE TRANSACTIONS ON COMMUNICATIONS, the IEEE COMMUNICATIONS LETTERS, and *Physical Communication* (Elsevier), and a Lead Guest Editor of the *EURASIP Journal on Wireless Communications and Networking*, Special Issue on Full-Duplex Radio: Theory, Design, and Applications. He has been serving as a TPC member of a number of flagship IEEE conferences. He was a TPC Co-Chair of the Workshop on Trusted Communications with Physical Layer Security of the IEEE GLOBECOM 2014 and a Publicity Chair of the Workshop on Full-Duplex Communications for Future Wireless Networks for the IEEE ICC 2017.

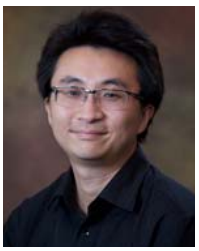

Jian Tang (SM'13) received the Ph.D. degree in computer science from Arizona State University in 2006. He is currently an Associate Professor with the Department of Electrical Engineering and Computer Science, Syracuse University. He has authored over 90 papers in premier journals and conferences. His research interests lie in the areas of wireless networking, big data, and cloud computing. He received the NSF CAREER Award in 2009, the 2016 Best Vehicular Electronics Paper Award from the IEEE Vehicular Technology Society, and best paper awards from the 2014 IEEE International Conference on Communications and the 2015 IEEE Global Communications Conference. He has been an Editor of the IEEE TRANSACTIONS ON WIRELESS COMMUNICATIONS since 2016, the IEEE TRANSACTIONS ON VEHICULAR TECHNOLOGY since 2010, and the IEEE INTERNET OF THINGS JOURNAL since 2013. He served as a TPC Co-Chair of the 2015 IEEE International Conference on Internet of Things and the 2016 International Conference on Computing, Networking and Communications.